https://doi.org/10.5194/cp-2021-40
Preprint. Discussion started: 21 April 2021

Climate of the Past Discussions

Simulation of the mid-Pliocene Warm Period using HadGEM3: Experimental design and results from model-model and model-data comparison

Charles J. R. Williams[1,6], Alistair A. Sellar[2], Xin Ren[1], Alan M. Haywood[3], Peter Hopcroft[4], Stephen J. Hunter[3], William H. G. Roberts[5], Robin S. Smith[6], Emma J. Stone[1], Julia C. Tindall[3], Daniel J. Lunt[1]

[1]School of Geographical Sciences, University of Bristol, UK
[2]Met Office Hadley Centre, UK
[3]School of Earth and Environment, University of Leeds, UK
[4]School of Geography, Earth and Environmental Sciences, University of Birmingham, UK
[5]Department of Geography and Environmental Sciences, Northumbria University, UK
[6]NCAS, Department of Meteorology, University of Reading, UK

*** Corresponding author address:**
School of Geographical Sciences,
University of Bristol,
University Road, Bristol, BS8 1SS
United Kingdom

Email: C.J.R.Williams@bristol.ac.uk

Short title: Model-model and model-data comparisons of the HadGEM3 mid-Pliocene simulation

Keywords: Palaeoclimate, Pliocene, model-data comparisons

https://doi.org/10.5194/cp-2021-40
Preprint. Discussion started: 21 April 2021

Climate of the Past Discussions
Open Access
EGU

ABSTRACT

Here we present the experimental design and results from a new mid-Pliocene simulation using the latest version of the UK's physical climate model, HadGEM3-GC31-LL, conducted under the auspices of CMIP6/PMIP4/PlioMIP2. Although two other paleoclimate simulations have been recently run using this model, they both focused on more recent periods within the Quaternary and therefore this is the first time this version of the UK model has been run this far back in time. The mid-Pliocene Warm Period, ~3 Ma, is of particular interest because it represents a time period when the Earth was in equilibrium with CO_2 concentrations roughly equivalent to those of today, providing a possible analogue for current and future climate change.

The implementation of the Pliocene boundary conditions is firstly described in detail, based on the PRISM4 dataset, including CO_2, ozone, orography, ice mask, lakes, vegetation fractions and vegetation functional types. These were incrementally added into the model, to change from a preindustrial setup to Pliocene conditions.

The results of the simulation are then presented, which are firstly compared with the model's pre-industrial simulation, secondly with previous versions of the same model and with available proxy data, and thirdly with all other models included in PlioMIP2. Firstly, the comparison with preindustrial suggests that the Pliocene simulation is consistent with current understanding and existing work, showing warmer and wetter conditions, and with the greatest warming occurring over high latitude and polar regions. The global mean surface air temperature anomaly at the end of the Pliocene simulation is 5.1°C, which is the 2nd highest of all models included in PlioMIP2 and is consistent with the fact that HadGEM3-GC31-LL has one of the highest Effective Climate Sensitivities of all CMIP6 models. Secondly, the comparison with previous generation models and with proxy data suggests a clear increase in global sea surface temperatures as the model has undergone development. Up to a certain level of warming, this results in a better agreement with available proxy data, and the "sweet spot" appears to be the previous CMIP5 generation of the model, HadGEM2-AO. The most recent simulation presented here, however, appears to show poorer agreement with the proxy data compared with HadGEM2, and may be overly sensitive to the Pliocene boundary conditions resulting in a climate that is too warm. Thirdly, the comparison with other models from PlioMIP2 further supports this conclusion, with HadGEM3-GC31-LL being one of the warmest and wettest models in all of PlioMIP2 and, if all the models are ordered according to agreement with proxy data, HadGEM3-GC31-LL ranks approximately halfway among them.

https://doi.org/10.5194/cp-2021-40
Preprint. Discussion started: 21 April 2021


Climate of the Past Discussions

1. INTRODUCTION

Model simulations of past climate states are useful because, among other aspects, they allow us to interrogate the mechanisms that have caused past climate change (Haywood *et al*. 2020, Lunt *et al*. 2021). They also give us a global picture of past climate variables (such as sea surface temperature, SST) that can only be reconstructed by geological data at specific locations, and of variables (such as upper atmospheric winds) that cannot be reconstructed by geological data at all. However, before models can be used in this way, it is important to validate them by comparing with geological data, where available, from the time periods of interest. Such model-data comparisons can also be useful for evaluating the model outside of the modern climate states that it was likely tuned to, thereby providing an independent assessment of the model that can be important for interpreting any future climate projections arising from the model (e.g. Zhu *et al*. 2020).

The mid-Pliocene Warm Period (mPWP, ~3 million years ago, hereafter referred to as the Pliocene) is an ideal climate state for such a model-data comparison because: i) there has recently been a concerted community effort to provide a synthesis of proxy SST reconstructions (McClymont *et al*. 2020); ii) community-endorsed boundary conditions exist which can be used to configure climate model simulations (Haywood *et al*. 2016); and iii) there is a wealth of previous model intercomparison projects (MIPs), with which model simulations can be compared and contrasted, that have been carried out with these recent boundary conditions (PlioMIP2, Haywood *et al*. 2020) and with previous versions of the boundary conditions (PlioMIP1, Haywood *et al*. 2013). The Pliocene is also a relatively warm period compared to both preindustrial conditions and those of today, with comparable CO_2 levels to today (McClymont *et al*. 2020, Salzmann *et al*. 2013), and so provides a climate state with similarities to those that might be expected in the future (Burke *et al*. 2018, Tierney *et al*. 2020).

PlioMIP2 was a community effort to carry out and analyse coordinated model simulations to explore mechanisms associated with Pliocene climate, and to evaluate multiple models with Pliocene proxy data. To date, 16 models have participated in PlioMIP2, and the results of this intercomparison and evaluation are described in Haywood *et al*. 2020 (hereafter abbreviated to H20). H20 first explored the large-scale features (global means, polar amplification and land-sea contrast) of temperature and precipitation in the simulations, finding a global ensemble mean warming of 3.2°C relative to preindustrial and a 7% increase in precipitation. There was a clear signal of polar amplification, but tropical zonal gradients remained largely unchanged compared with preindustrial. Compared with proxies from Foley and Dowsett (2019), the SSTs in the tropics were broadly consistent in the models and data, and in the Atlantic the polar amplification was better represented by the models compared with previous model-data comparisons such as those from PlioMIP1. Recent studies using the PlioMIP2 ensemble have explored other aspects of the model simulations, such as ocean circulation

https://doi.org/10.5194/cp-2021-40
Preprint. Discussion started: 21 April 2021


Climate of the Past Discussions

(Zhang *et al*. 2021) and the African monsoon (Berntell *et al*., in review). It is of interest to evaluate simulations from additional models as they become available, and that is what we do here, presenting results from a new model, HadGEM3-GC31-LL, for the Pliocene. This is of particular interest because HadGEM3-GC31-LL is a Coupled Model Intercomparison Project Phase 6 (CMIP6) "high Effective Climate Sensitivity (ECS)" model (Zelinka *et al*. 2020), with a climate sensitivity to CO_2 doubling of more than 5°C (Andrews *et al*. 2019). Only one other model in CMIP6, CanESM5, has a higher climate sensitivity (5.64°C compared with 5.55°C). HadGEM3-GC31-LL is also of interest because it represents the third generation of UK Met Office model that has participated in PlioMIP (Bragg *et al*. 2012, Tindall and Haywood 2020, Hunter *et al*. 2019), allowing us to assess how much, if any, progress has been made in simulating the Pliocene with the UK family of models.

In this paper we address 3 main questions:

1) What are the large-scale features of the Pliocene climate produced by HadGEM3-GC31-LL?
2) To what extent has the development of new boundary conditions and more complex models led to improvements in the simulation of the Pliocene by UK Met Office models?
3) How does HadGEM3-GC31-LL compare with other models participating in PlioMIP2?

Section 2 of this paper describes HadGEM3-GC31-LL, how the PlioMIP2 boundary conditions were implemented in the model, and the experimental design of the model. Section 3 presents the large-scale features of the Pliocene in HadGEM3-GC31-LL, and Section 4 compares the HadGEM3-GC31-LL simulation with proxy data and previous generations of the same UK model, and with other PlioMIP2 models.

2. MODEL AND EXPERIMENT DESIGN

2.1. Naming conventions and terminology

Consistent with CMIP nomenclature, when the simulation is spinning up towards atmospheric and oceanic equilibrium, with initially incomplete boundary conditions, it is referred to as the 'Spin-up phase' and is only briefly presented here. In contrast, once all required boundary conditions were implemented, the results themselves are taken from the end of the simulation, referred to here as the 'Production run'. Here, results are based on the final 50-year climatology of this production run. Concerning geological intervals, the preindustrial and mid-Pliocene Warm Period are referred to as the PI and Pliocene, respectively. In contrast, concerning the model simulations using HadGEM3-GC31-LL, consistent with CMIP6 they are referred to as the *piControl* and *mPWP* simulations, respectively. We also make use of the naming convention of Haywood *et al*. 2016, hereafter abbreviated to H16), including the nomenclature Ex^c (where c is the concentration of CO_2 in ppmv, and x are any boundary conditions which are Pliocene as opposed to PI, which can be any or none of

https://doi.org/10.5194/cp-2021-40
Preprint. Discussion started: 21 April 2021


Climate of the Past Discussions

o = orography, v = vegetation and i = ice sheets). So, for example, Eov^{500} would be an experiment using Pliocene orography and vegetation and with CO_2 at 500 ppmv, but with preindustrial ice sheets.

2.2. Model description

2.2.1. HadGEM3-GC31-LL

The model presented here is the Global Coupled (GC) 3.1 configuration of the UK's physical climate model, HadGEM3-GC31-LL, which is the "CMIP6-class" UK Met Office physical climate model. The *piControl* simulation for this model was conducted elsewhere as part of CMIP6, and is used here for comparative purposes; see Williams *et al*. (2017), Kuhlbrodt *et al*. (2018) and Menary *et al*. (2018) for further details on HadGEM3-GC31-LL and its *piControl* simulation. The *mPWP* simulation presented here was run with identical components to those used in other CMIP6/PMIP4 simulations using this model, namely the *midHolocene* and *lig127k* simulations (Williams *et al*. 2020). The full title for this configuration is HadGEM3-GC31-LL N96ORCA1 UM10.7 NEMO3.6 (hereafter referred to as HadGEM3). The model was run using the Unified Model (UM), version 10.7, and included the following components: i) Global Atmosphere (GA) version 7.1, with an N96 atmospheric spatial resolution (approximately 1.875° longitude by 1.25° latitude) and 85 vertical levels; ii) NEMO ocean version 3.6, including Global Ocean (GO) version 6.0 (ORCA1), with an isotropic Mercator grid which, despite varying in both meridional and zonal directions, has an approximate spatial resolution of 1° by 1° and 75 vertical levels; iii) Global Sea Ice (GSI) version 8.0 (GSI8.0); iv) Global Land (GL) version 7.0, comprising the Joint UK Land Environment Simulator (JULES); and v) the OASIS3 MCT coupler. All of the above individual components are summarised by Williams *et al*. (2017) and detailed individually by a suite of companion papers (see Walters *et al*. 2017 for GA7 and GL7, Storkey *et al*. 2017 for GO6 and Ridley *et al*. 2017 for GSI8). A summary of the major changes in HadGEM3 and their impacts on the climate, relative to its most recent predecessor (HadGEM2), are given in Williams *et al*. (2020). Here, the *mPWP* simulation was run on NEXCS, which is a component of the Cray XC40 located at the UK Met Office. NEXCS is a partition of the UK Met Office's platform, Monsoon, on which the *piControl* simulation was run, thereby avoiding the potential caveat discussed in Williams *et al*. (2020) concerning different computing platforms.

2.2.2. Other models

Details of the other models discussed here, namely previous generations of the same UK model and all of those included in PlioMIP2, are included in the Supplementary Material.

2.3. Full Pliocene experiment design

https://doi.org/10.5194/cp-2021-40
Preprint. Discussion started: 21 April 2021


Climate of the Past Discussions

For the most part, the *mPWP* simulation presented here follows the protocol given in H16, discussed below. The main difference is that we do not modify the land-sea mask (LSM), due to technical challenges of modifying the ocean LSM and coupling it to the atmosphere.

2.3.1. Greenhouse gas atmospheric concentrations, aerosol emissions and ozone

Following H16, atmospheric CO_2 concentration was modified in the *mPWP* simulation, from 280 to 400 ppmv. All other greenhouse gases, such as CH_4, N_2O and O_2, were kept as in the *piControl* simulation. Likewise, aerosol emissions (e.g. organic- and black-carbon fossil fuels) and their resulting oxidants were kept as in the *piControl* simulation, consistent with previous paleoclimate simulations with this model (Williams *et al*. 2020).

Under strong surface warming, the thermal tropopause rises. In simulations with prescribed ozone concentration it is important that the thermal tropopause remains below the ozone tropopause, in order to avoid unphysical feedbacks associated with increasing cold point temperature (see, for example, Hardiman *et al*. 2019). For this reason, ozone from the *1pctCO₂* simulation of the UK Earth System Model (UKESM1, see Sellar *et al*. 2019), in which CO_2 concentrations are increased relative to 1850 levels at 1% per year, was prescribed here. UKESM1 uses the same physical climate configuration as HadGEM3, but interactively simulates ozone chemistry. The ozone was taken from a 10-year period of this UKESM1 simulation (years 51-60), during which the mean surface temperature was approximately 2°C warmer than the *piControl* simulation. The value of 2°C was chosen as a compromise between raising the ozone tropopause enough to avoid inconsistency with the thermal tropopause, without introducing significant changes in ozone forcing relative to the *piControl*. The impact of the ozone modification could be explored in future work, for example by using an ozone profile from a UKESM1 simulation with a higher mean surface temperature (more consistent with the HadGEM3 Pliocene warming, see Section 3), or by using the methodology outlined in Hardiman *et al*. (2019), which was used for the CMIP6 Shared Socioeconomic Pathway (SSP) scenario simulations with HadGEM3.

2.3.2. Changes to boundary and initial conditions

2.3.2.1. Palaeogeography (including land-sea mask, orography and bathymetry)

The *mPWP* simulation used an identical LSM to the *piControl* simulation, which H16 allows if necessary. This differs from both the standard and enhanced LSMs provided by H16 (accessible, with all other required boundary conditions, from the US Geological Survey's PlioMIP2 website, http://geology.er.usgs.gov/egpsc/prism/7_pliomip2.html), in that in both of these the gateways in the Bering Sea, the Canadian Archipelago and Hudson Bay are closed, whereas in the HadGEM3 simulations only the Canadian Archipelago/Hudson Bay gateway is closed; the Bering Strait is open

https://doi.org/10.5194/cp-2021-40
Preprint. Discussion started: 21 April 2021

Climate of the Past Discussions
Open Access
EGU

(see Supplementary Material, Fig. S1). Likewise, the bathymetry used here is also identical to the *piControl* simulation, for the same reasons.

The orography used in the *mPWP* simulation, however, does follow the protocol of H16. Here, an anomaly is firstly created by subtracting the PRISM4 modern orography from the PRISM4 Pliocene orography and then, after having been re-gridded to the model's own resolution, adding this to the model's existing orography (see Section 2.3.2 in H16). The results are shown in Figure 1, where the PRISM4 anomaly shows the largest changes are occurring over Greenland and Antarctica, with smaller changes over the Himalayas, North America and Africa (Fig. 1a). When added to HadGEM3's existing orography (Fig. 1b), the changes result most obviously in a lowering of orography over Greenland, western and eastern Antarctica, and a raising of orography over central Antarctica (Fig. 1c). Due to an early model instability relating to the steep orographic gradients in western Antarctica, this region was smoothed in the final simulation (Fig. 1c).

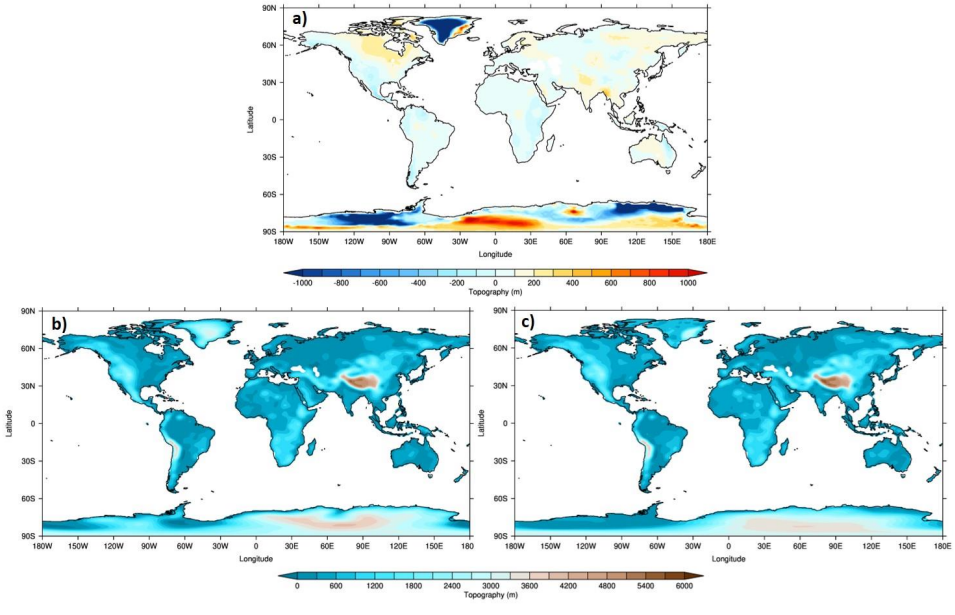

Figure 1 - Changes to topography in HadGEM3 *mPWP* simulation. a) PRISM4 anomaly; b) Original field used in HadGEM3 *piControl*; c) New field used in HadGEM3 *mPWP*, with smoothed topography over western Antarctica (final version, used in simulation)

2.3.2.2. Vegetation fractions (including urban, lakes and ice)

As part of its GL configuration, both the *piControl* and *mPWP* simulations used the community land surface model, JULES; see Best *et al*. 2011, Clark *et al*. 2011, Walters *et al*. 2019). In this land surface model, sub-gridscale heterogeneity is represented by a tile approach (Essery *et al*. 2003), in

https://doi.org/10.5194/cp-2021-40
Preprint. Discussion started: 21 April 2021

Climate of the Past Discussions
Open Access
EGU

234 which each grid box over land is divided into five vegetated plant functional types (PFTs): broadleaf
235 trees (BLT), needle-leaved trees (NLT), temperate C3 grass, tropical C4 grass and shrubs. In addition
236 to these, there are four non-vegetated PFTs: urban areas, inland water (or lakes), bare soil and land
237 ice. This division of grid box into PFTs is consistent with both of the model's predecessors (see
238 Supplementary Material). With the exception of the urban tile, which was kept as PI to be consistent
239 with previous paleoclimate simulations with this model (Williams *et al*. 2020), all of these PFTs were
240 modified in the *mPWP* simulation.
241
242 The US Geological Survey's PRISM4 (Pliocene Research, Interpretation and Synoptic Mapping v4;
243 see Dowsett *et al*. 2016) vegetation reconstruction from Salzmann *et al*. (2008) was used, provided as
244 a megabiome reconstruction in PlioMIP2 (H16). This can be seen in Figure 2, where there are ten
245 listed megabiomes corresponding to those used in Harrison and Prentice 2003: tropical forest, warm-
246 temperate forest, savanna and dry woodland, grassland and dry shrubland, desert, temperate forest,
247 boreal forest, tundra, dry tundra and land ice.

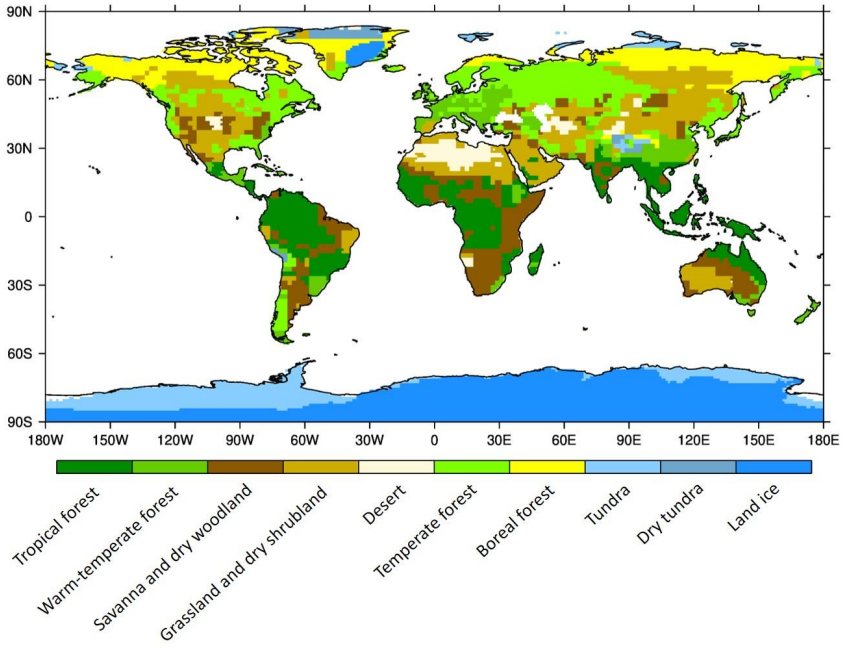

248
249 Figure 2 - Ten megabiomes from PlioMIP2 used create the nine PFTs used in HadGEM3 *mPWP* simulation
250
251
252
253

https://doi.org/10.5194/cp-2021-40
Preprint. Discussion started: 21 April 2021


Climate of the Past Discussions
Open Access
EGU

To translate the megabiomes from PRISM into the PFTs used by the model, a lookup table was therefore required. Minimum and maximum bounds for each megabiome were firstly obtained, based on values from Crucifix *et al*. 2005, and then estimates were made for each PFT within these bounds by mapping the prindustrial megabiomes onto the preindustrial PFT in HadGEM3; the resulting lookup table is shown in the Supplementary Material (Table S1). In this table, for example, each land grid point with the megabiome "Tropical forest" is divided amongst the model PFTs as 92% BLT, 5% bare soil, 2% tropical C4 grasses and 1% shrubs. The resulting 9 PFTs used in the *mPWP* simulation, as well as those from the original *piControl*, are shown in Figure 3. The largest fractional increases, relative to the *piControl*, occur for broadleaf trees and needleleaf trees (18% and 5%, respectively; Fig. 3a and b) and the largest decreases occur for temperate C3 grass and land ice (15% and 5%, respectively; Fig. 3c and i).

https://doi.org/10.5194/cp-2021-40
Preprint. Discussion started: 21 April 2021

Climate of the Past Discussions
Open Access
EGU

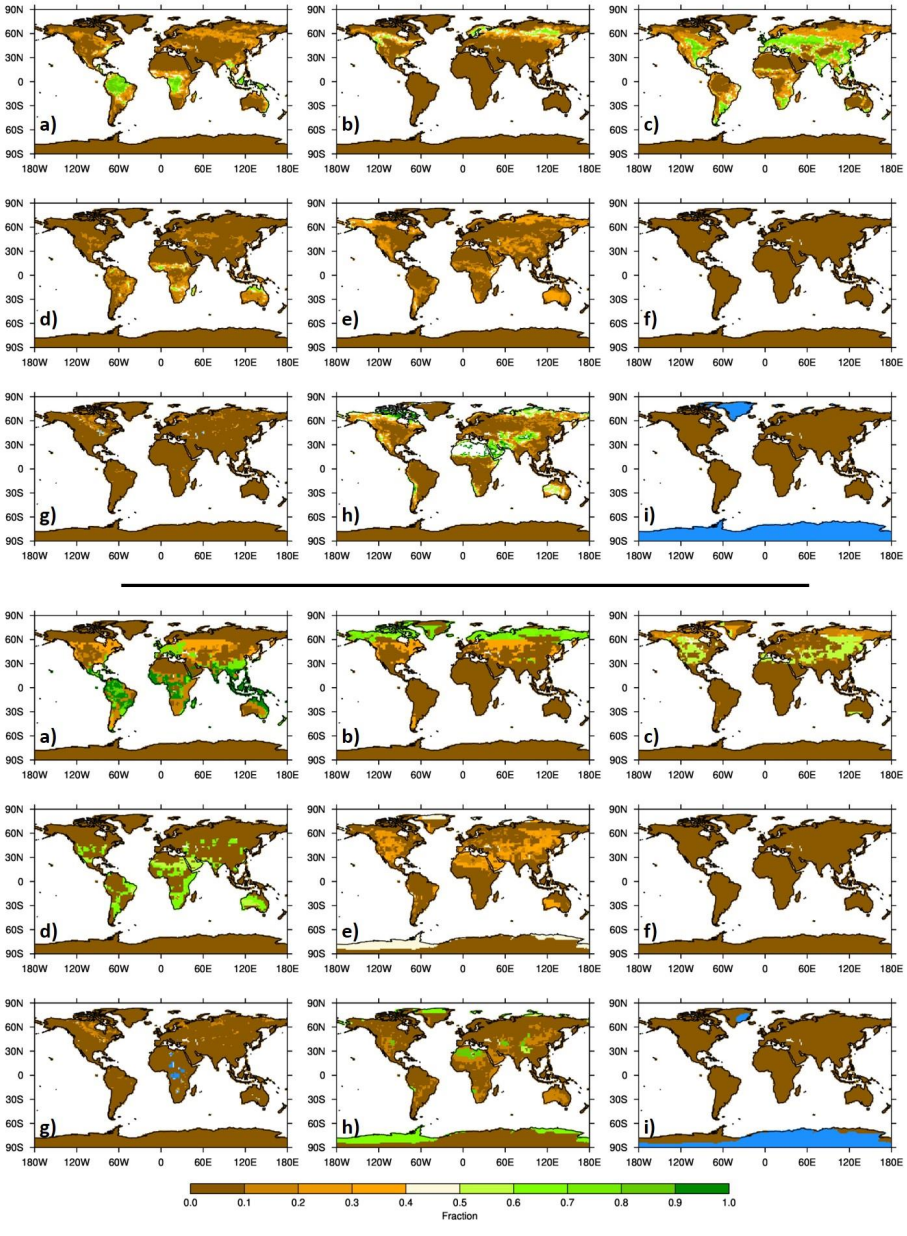

Figure 3 - Nine PFTs used in HadGEM3. Top half: *piControl* simulation, bottom half: *mPWP* simulation. Values in brackets show global mean differences (*mPWP* - *piControl*), expressed as a percentage. a) broadleaf trees (18%); b) needle-leaved trees (5%); c) temperate C3 grass (-15%); d) tropical C4 grass (6%); e) shrubs (3%); f) urban areas (no change); g) inland water (1%); h) bare soil (-12%); i) land ice (-5%)

https://doi.org/10.5194/cp-2021-40
Preprint. Discussion started: 21 April 2021


Climate of the Past Discussions

2.3.2.3. Vegetation functional types

Alongside the vegetation fractions, both the *piControl* and *mPWP* simulations included two monthly-varying vegetation functional types, namely leaf area index (LAI) and canopy height, both of which are associated with each of the five vegetated PFTs. Given that no information was available from the PRISM vegetation reconstruction concerning these fields, two methods were used to create Pliocene LAI and canopy height. For LAI, a seasonally and latitudinally varying function was created from the zonal means of the *piControl* (Figure 4), and used to build a new field for the Pliocene, for each month and each PFT (see Fig. 4f and g for an example of the original *piControl* and the Pliocene newly-created field, respectively, both showing LAI for BLT during January). This is because, in the *piControl*, LAI varies both in time (i.e. seasonally) and space. Note that although LAI does go to zero in the *piControl*, this was not allowed in the *mPWP* simulation because the Pliocene does have some vegetation at high latitudes (see Figure 3); these functions were therefore increased by x (where x = the mean of the ten grid points containing the lowest LAI), such that there is never zero LAI. In contrast, canopy height in the *piControl* does not vary monthly, and has little variation spatially, therefore canopy height in the *mPWP* simulation is set to the global mean of the *piControl* (see Supplementary Material Fig. S2).

https://doi.org/10.5194/cp-2021-40
Preprint. Discussion started: 21 April 2021

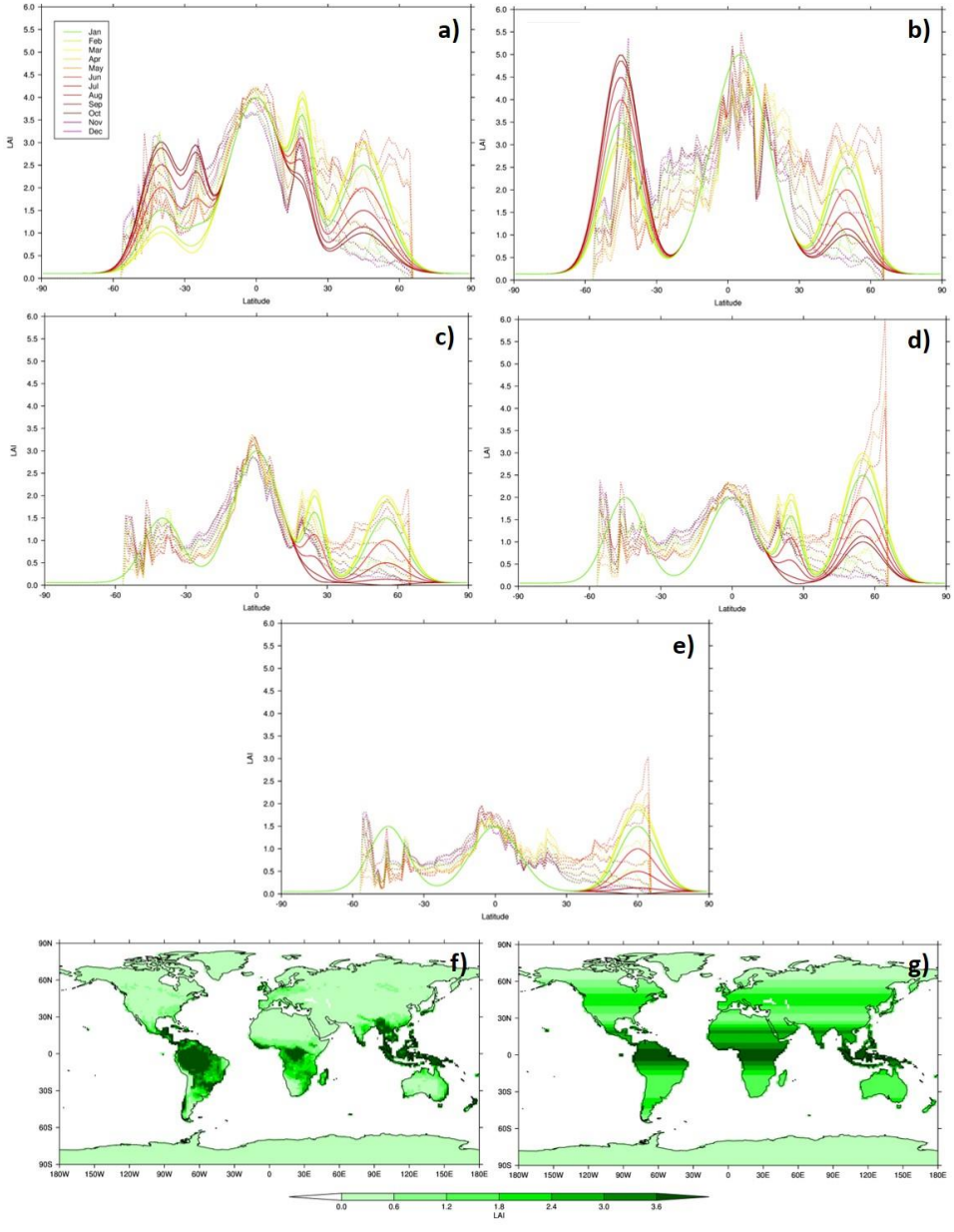

Figure 4 – LAI used in HadGEM3, for each month and PFT. Dashed lines show zonal mean from *piControl* simulation, solid lines show seasonally and latitudinally varying function of this zonal mean, used in *mPWP* simulation. a) broadleaf trees; b) needle-leaved trees; c) temperate C3 grass; d) tropical C4 grass; e) shrubs; f) example of final functional types used in *piControl* simulation (LAI for broadleaf trees, January); g) same as f) but for the *mPWP* simulation

https://doi.org/10.5194/cp-2021-40
Preprint. Discussion started: 21 April 2021


Climate of the Past Discussions

297 ***2.3.2.3. Soil properties and snow depth***

298 Under newly-created land ice based on the new Pliocene ice mask (i.e. in regions where there is no ice
299 in the *piControl* but ice the *mPWP* simulation), soil parameters, soil dust properties and snow depth
300 were set to be appropriate values for existing ice regions i.e. whatever these values are under ice in the
301 *piControl* simulation are applied to the newly-created ice regions in the *mPWP* simulation.
302
303 Conversely, and more importantly in this context (as the Pliocene represents an overall removal of
304 ice), under newly-exposed land based on the new Pliocene ice mask (i.e. in regions where there is ice
305 in the *piControl* but no ice in the *mPWP* simulation, primarily over Greenland and western
306 Antarctica), the dominant vegetation fractions in these regions were firstly identified. In this case, the
307 dominant fractions were 40% shrubs and 60% bare soil. Then, grid points containing this vegetation
308 balance in the *piControl* were identified, and the soil parameters, soil dust properties and snow depth
309 values at these points were averaged. This average value, for each of the above fields, was lastly
310 inserted back into the *mPWP* simulation's newly-exposed grid points; it is acknowledged that this
311 introduces new dust emissions source regions, which may well impact the resulting Pliocene climate
312 state.
313
314 ***2.3.2.4. Initial conditions***
315 The same method as that applied to soil properties was also applied to other initial conditions, such as
316 such as soil moisture and soil temperature at 4 levels of depth. These fields contain monthly varying
317 values, therefore appropriate timings were considered e.g. if the majority of grid points with the above
318 balance were in the Northern Hemisphere, then initial conditions during Northern Hemisphere
319 summer were used for newly-exposed regions in Greenland (and likewise during Southern
320 Hemisphere summer for newly-exposed regions in Antarctica). For the soil temperature field and
321 particularly at upper levels, this process resulted in sharp temperature gradients across western
322 Antarctica, therefore the field was spatially smoothed so that the gradients were more consistent with
323 those in the *piControl*. Examples of the above soil-related fields are shown in Figure 5 for an
324 example month and vertical level. A complete list of the soil parameters and soil dust properties, and
325 how each were changed relative to the *piControl*, are shown in the Supplementary Material (Fig. S3
326 and Fig. S4, respectively).
327
328 Outside of the ice regions (i.e. outside Greenland and Antarctica), in the *mPWP* simulation the above
329 soil-related fields were kept identical as in the *piControl*.

https://doi.org/10.5194/cp-2021-40
Preprint. Discussion started: 21 April 2021

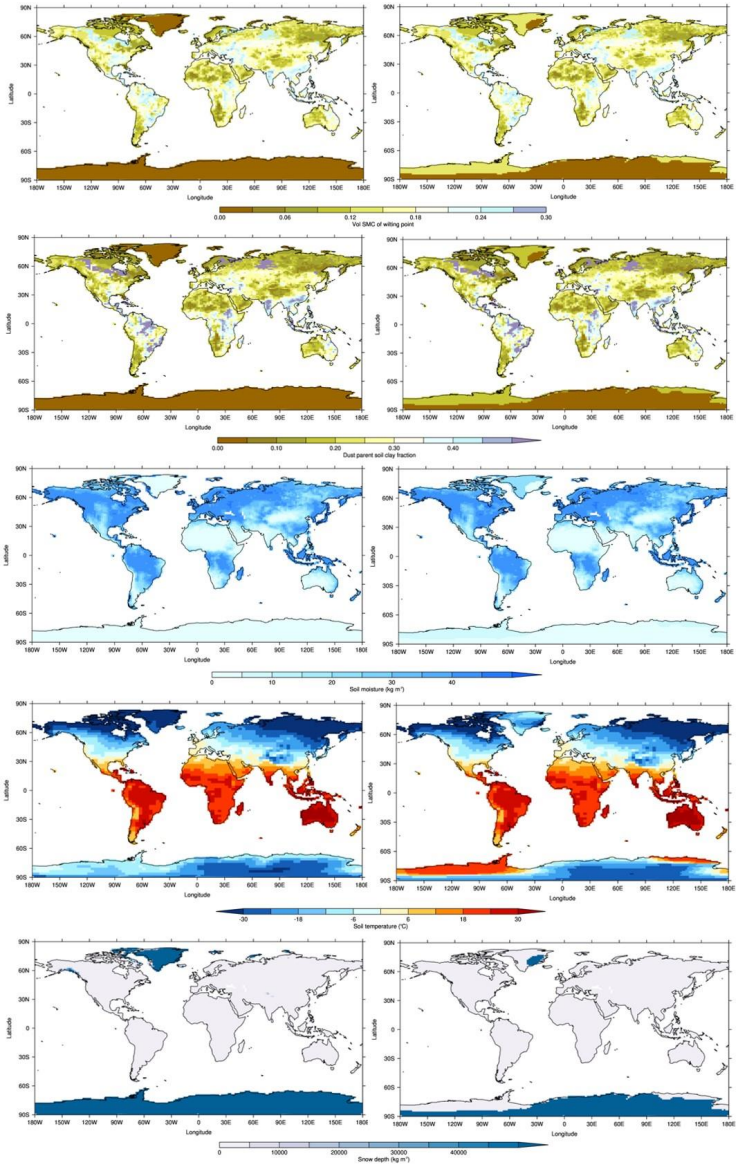

Figure 5 – Examples of soil-related fields used in HadGEM3 (complete list of fields shown in Supplementary Material Fig. S3 and Fig. S4). Left-hand column: *piControl* simulation, right-hand column: *mPWP* simulation. First row: Soil parameters (example shows Volumetric soil moisture content at wilting point); Second row: Soil dust properties (example shows Dust parent soil clay fraction); Third row: Soil moisture (example shows January, top-level); Fourth row: Soil temperature (example shows January, top-level); Last row: Snow depth

2.3.3. Changes to input parameters

A small number of model input parameters were changed in the *mPWP* simulation, to make the model more stable under the Pliocene boundary conditions. Firstly a parameter governing the implicit solver

https://doi.org/10.5194/cp-2021-40
Preprint. Discussion started: 21 April 2021


Climate of the Past Discussions

for unstable boundary layers was increased, and secondly three parameters for the treatment of canopy snow were made consistent between BLT and NLT. The same parameter changes will be included in the subsequent version of the physical model (GC4), in order to address occasional model failures which were seen following the release of GC3.1. They will be described in more detail in a GC4 model documentation paper, however testing of those changes for GC4 has found that they have no detectable impact on model climatology.

2.4. Modified *piControl* simulation

Given that the official CMIP6 *piControl* simulation did not use the aforementioned model input parameter changes, a slightly modified version of this simulation was re-run (simulation ID: u-bq637), identical to the *piControl* other than these parameter changes (hereafter referred to as the *piControl_mod* simulation). This was run for 200 years, and the last 50-year climatology is considered here in Sections 3 and 4.

3. LARGE-SCALE FEATURES OF HADGEM3

3.1. Spin-up phase

Consistent with other paleoclimate model experiments, the simulation should be run for as long as possible to allow the model to reach a state of equilibrium, before the climatology is calculated over the last 30, 50 or 100 years (Lunt *et al*. 2017). With this model, however, running for the thousands of years ideally needed (especially important in obtaining oceanic equilibrium) was unfeasible given time and resource constraints. By the end of the simulation, therefore, there was a total of 576 years for the *mPWP* simulation, 526 of which are considered spin-up and 50 of which form the final climatologies; this is approximately consistent with the 652 years of spin-up used by Menary *et al*. (2018).

3.1.1. Evolution of mPWP simulation

The HadGEM3 *mPWP* simulation was run in multiple parts, each starting from the endpoint of the last, and each introducing additional boundary conditions so as to gradually move from PI conditions to full Pliocene conditions. The *mPWP* simulation was started from the endpoint of the CMIP6 *piControl* simulation, specifically the last part of its spin-up phase (u-aq853), consistent with other CMIP6 HadGEM3 paleoclimate simulations such as those of the mid-Holocene and Last Interglacial periods (see Williams *et al*. 2020). The evolution of the *mPWP* simulation is shown in Figure 6, where each stage is labelled and the resulting impact on the global mean 1.5 m air temperature is shown. The first part of the *mPWP* simulation (u-bq448) is a straight copy of the CMIP6 *piControl* production run (u-ar766), with no modifications other than increasing the atmospheric CO_2 to 400 ppmv; identical, therefore, to an E^{400} experiment following the naming convention of H16. This ran for ~20 model years, before branching off to a new suite (u-br005) and introducing atmospheric ozone

https://doi.org/10.5194/cp-2021-40
Preprint. Discussion started: 21 April 2021

appropriate for Pliocene conditions and Pliocene orography (see Section 2.3.1 and 2.3.2, respectively). This ran for ~60 model years, before branching off to a new suite (u-br871) and introducing a Pliocene-appropriate ice mask along with appropriate values for soil parameters, soil dust, soil moisture, soil temperatures and snow depth over these newly created ice regions (see Section 2.3.2); this, therefore would be the Eoi^{400} experiment following the naming convention of H16. It should be noted, however, that at this stage this naming convention is not strictly consistent with that used by H16, because they specify that orography, lakes and soils should be modified in unison, and therefore *o* signifies changes to orography, bathymetry, land-sea mask, lakes and soils together. In contrast, at this stage of the simulation, most boundary conditions are consistent with the experimental design of H16, except vegetation, soils in non-ice regions and lakes. This ran for ~280 model years (during which time the task of creating appropriate Pliocene vegetation was completed), before branching off to a new suite (u-bv241) and introducing a minor parameter change to allow inclusion of the Pliocene vegetation (see Section 2.3.3), as well as the full Pliocene vegetation fractions. This ran for a further ~60 years, to check the stability of the model in response to the vegetation change, before branching off to a new and final suite (u-bv963), in which the full Pliocene vegetation functional types were introduced. This ran for 150 years, with the final climatology (presented here in Section 3 and 4) being taken from the last 50 years i.e. allowing a 100-year buffer between the final update to the model and the actual results.

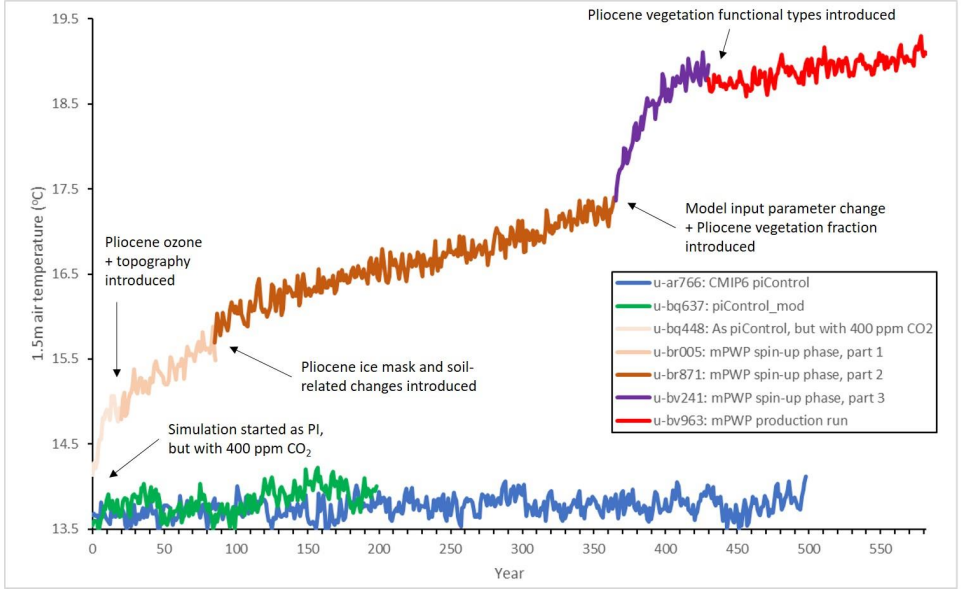

Figure 6 – Annual global mean 1.5 m air temperature from the HadGEM3 *mPWP* spin-up phase and production run, as well as the CMIP6 *piControl* and the *piControl_mod*. Labels show introduction of each new Pliocene element. Climatologies discussed here are taken from final 50 years of each simulation. See Williams *et al*. (2020) for the *piControl* spin-up phase that preceded these simulations.

https://doi.org/10.5194/cp-2021-40
Preprint. Discussion started: 21 April 2021

Climate of the Past Discussions
Open Access
EGU

401 ***3.1.2. Atmospheric and oceanic equilibrium of the mPWP simulation***

402 Concerning atmospheric equilibrium, Table 1 shows summary statistics for annual global mean 1.5 m
403 air temperature and net top of atmosphere (TOA) radiation from the last 50 years of the *mPWP*
404 simulation, compared to both the *piControl* and *piControl_mod* simulations; see Figure 6 for the
405 entire timeseries of Pliocene 1.5 m air temperature, and Figure S5 in the Supplementary Material for
406 the TOA radiation equivalent.

Variable	*piControl*	*piControl_mod*	*mPWP*
1.5m air temperature (°C)	0.51	-0.47	0.34
TOA radiation (W m^2)	0.02	-0.2	-0.17
OceTemp (°C)	0.03	0.04	0.21
OceSal (psu)	0.0004	-0.0002	-0.004

407

408 Table 1 - Centennial trends (calculated via a linear regression) in global mean measures of climate equilibrium over the last
409 50 years of the simulations, adapted from Menary *et al*. (2018) to include the CMIP6 *piControl*, *piControl_mod* and *mPWP*
410 simulations. Negative TOA radiation = net radiation flux is downward

411

412 Although the *mPWP* simulation is clearly warming considerably during the ~500 year run (and
413 especially when Pliocene vegetation is introduced), with trends of 0.77°C century^{-1}, it levels off over
414 the final 50 years, with trends of 0.34°C century^{-1} (Table 1). These values are higher than those
415 considered by Menary *et al*. (2018) to be acceptable for equilibrium (0.03°C century^{-1}), however
416 given time and resource constraints it was not possible to run the simulation further. The spatial
417 patterns of these trends, shown in Figure S6 in the Supplementary Material, shows the majority of the
418 warming occurring over high latitude regions in both Hemispheres, related to the removal of the ice
419 sheets and sea ice loss. The TOA radiation centennial trends are negative throughout the *mPWP*
420 simulation (-0.02 W m^2 century^{-1} over the whole ~500 years) and actually decreases over the last 50
421 years to -0.17 W m^2 century^{-1} (Table 1, where negative TOA radiation = net radiation flux is
422 downward).

423

424 As an example of oceanic equilibrium, Table 1 also shows summary statistics for full depth annual
425 global mean ocean temperature and salinity (OceTemp and OceSal, respectively) from the end of the
426 *mPWP* simulation, compared to both the *piControl* and *piControl_mod* simulations; see Figure S7 in
427 the Supplementary Material for the Pliocene timeseries. OceTemp is steadily increasing throughout
428 the *mPWP* simulation, and likewise OceSal is steadily decreasing (Fig. S7). The long-term trends,
429 Table 1, provide similar conclusions to the atmosphere, with for example centennial temperature
430 trends of 0.21°C century^{-1} being much higher than the PI simulations (0.03°C century^{-1} and 0.04°C
431 century^{-1} for the *piControl* and *piControl_mod*, respectively). Although these values again do not

https://doi.org/10.5194/cp-2021-40
Preprint. Discussion started: 21 April 2021


Climate of the Past Discussions

meet the criteria of Menary *et al*. (2018) for oceanic equilibrium, given the aforementioned computational cost of this model it was not possible to run the simulations further; this is even more true in the ocean, which would require many thousands of years of model simulation to reach equilibrium. This compromise has been equally necessary for other computationally expensive models conducting paleoclimate simulations.

3.2. Simulation comparison: *mPWP* versus *piControl_mod* climatologies

Here the focus is on mean differences between the HadGEM3 *mPWP* simulation and its corresponding modified PI simulation, *piControl_mod* (Section 2.4). All of the following discussion and figures relate to climatologies calculated over the last 50 years of the simulations, and all are anomalies i.e. Pliocene - PI. Annual and seasonal mean summer/winter 1.5 m air temperature (hereafter referred to as near-surface air temperature, SAT) anomalies are shown in Figure 7. The annual global mean SAT anomaly for this 50-year climatology is 5.1°C. Warming relative to the PI is evident throughout the year and globally, but more so over: i) landmasses (6.8°C and 4.5°C for the annual mean SAT over land and ocean, respectively); ii) the Northern Hemisphere (8.5°C and 6.3°C for annual mean SAT in the Northern and Southern Hemisphere extratropics (>45°), respectively); and iii) over high latitudes (>60°) of both hemispheres (10.9°C and 8.5°C for the Northern and Southern Hemisphere, respectively, and exceeding 12°C in some places). Over the tropics (20°N-20°S) the amount of warming is less than at higher latitudes, but the Pliocene is still much warmer than the PI with annual mean SAT anomalies of 4.6°C and 3.7°C when averaged over tropical land and ocean, respectively. This global and regional warming is consistent with, albeit slightly warmer than, other work, namely the results from PlioMIP1 (Haywood *et al*. 2013) and PlioMIP2 (H20; see Section 4.2). The majority of the annual mean warming (Fig. 7a) in Northern Hemisphere high latitudes is accounted for during that hemisphere's winter (December-February, DJF) with a mean warming of 15°C (Fig. 7b), and likewise the majority of the annual mean warming in Southern Hemisphere high latitudes is accounted for during that hemisphere's winter (June-August, JJA) with a mean warming of 10.6°C (Fig. 7c). If the entire hemisphere, rather than >60°, is considered, then this greater winter contribution to the annual mean is still true, although less so (e.g. 5.6°C, 6.1°C and 5.4°C for the annual, DJF and JJA means respectively in the Northern Hemisphere). The regions of polar SAT increases, and seasonal variation, are likely explained by the changes in sea ice, shown in Figure 8 (for the absolute values in sea ice fraction, see Fig. S8 in the Supplementary Material). Reductions in sea ice are shown throughout the year in both hemispheres, consistent with previous work (e.g. Cronin *et al*. 1993, Howell *et al*. 2016, Moran *et al*. 2006, Polyak *et al*. 2010). Here, although a reduction in annual sea ice sea ice (of up to 70%) is clear (Fig. 8a), at the seasonal timescale the largest loss (exceeding 70% in some places, such as the polar Arctic) is seen during each hemisphere's winter; as shown by Figure 7b-c, the regions/timings of maximum warming correspond well to the regions/timings of maximum sea ice loss.

https://doi.org/10.5194/cp-2021-40
Preprint. Discussion started: 21 April 2021

Climate of the Past Discussions
Open Access
EGU

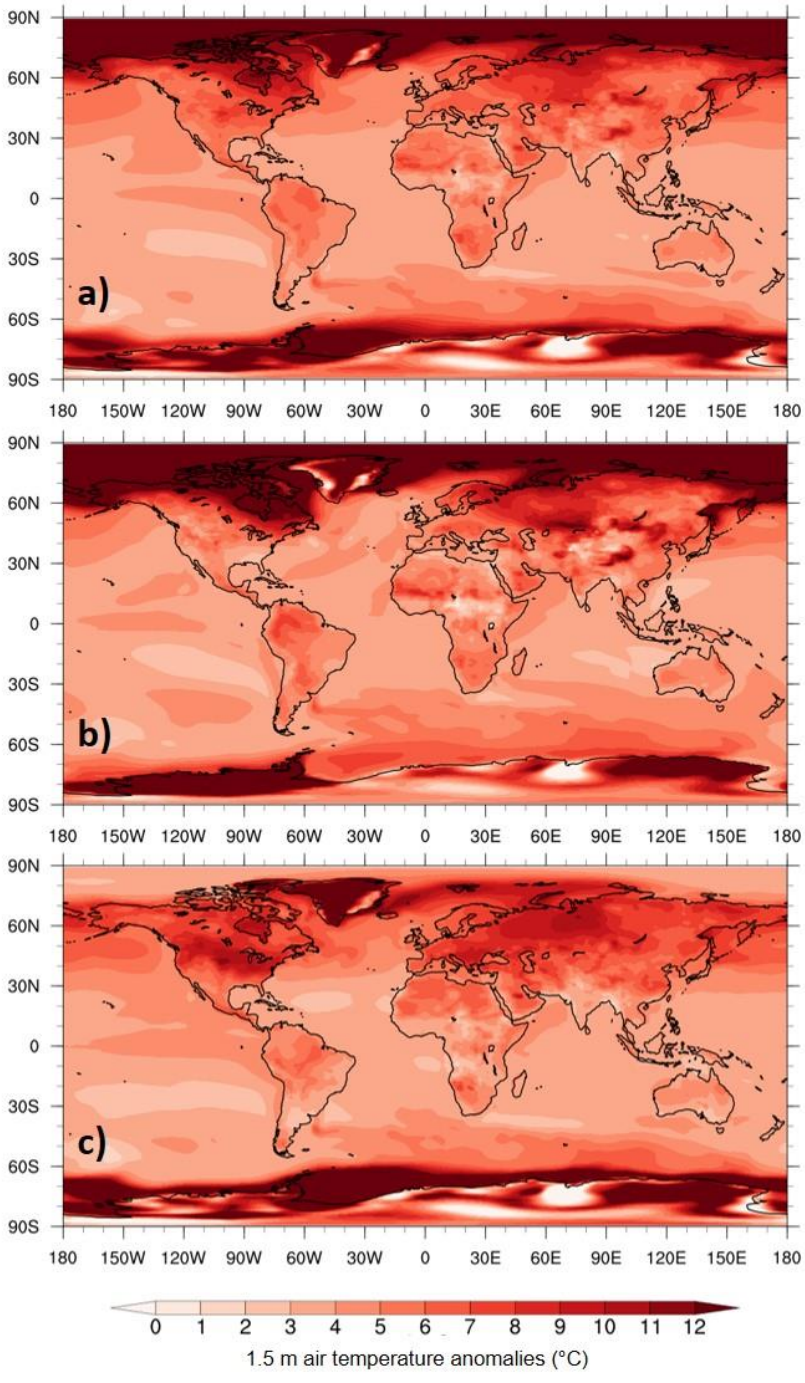

469

470 Figure 7 – 1.5 m air temperature climatology differences (*mPWP – piControl_mod*) from HadGEM3. a) Annual; b) DJF; c)
471 JJA

https://doi.org/10.5194/cp-2021-40
Preprint. Discussion started: 21 April 2021

Climate of the Past Discussions
Open Access
EGU

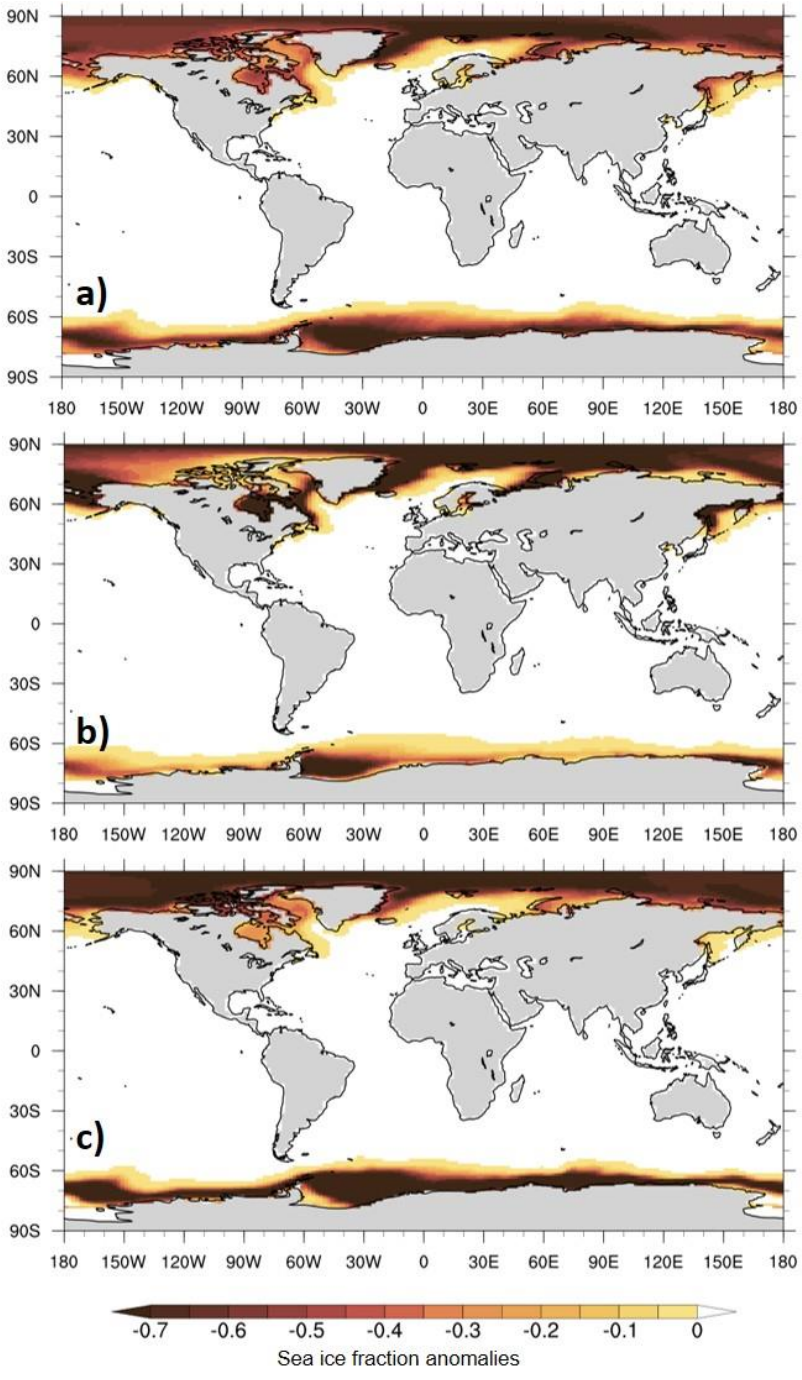

Figure 8 – Sea ice fraction climatology differences (*mPWP – piControl_mod*) from HadGEM3. a) Annual; b) DJF; c) JJA

https://doi.org/10.5194/cp-2021-40
Preprint. Discussion started: 21 April 2021


Climate of the Past Discussions

Annual and seasonal mean surface daily precipitation anomalies are shown in Figure 9. The annual global mean precipitation anomaly for this 50-year climatology is 0.34 mm day^{-1}. In addition to the precipitation increases at high latitudes at the annual timescale (Fig. 9a), which are again mostly accounted for by changes during the Northern and Southern Hemisphere's winter (Fig. 9b and c, respectively), the largest change relative to the PI is a northward displacement of the ITCZ, with all timescales showing wetter conditions over oceans to the North of the equator and drier conditions over oceans to the South of the equator. This is similar to work by Li *et al*. (2018), who suggested a poleward movement of Northern Hemisphere monsoon precipitation in PlioMIP1. There is also a noticeable enhancement of monsoon systems such as the East Asian and West African monsoon, consistent with previous work (e.g. Zhang *et al*. 2013, 2016). In some places, these changes exceed ~2 mm day^{-1}, geographically consistent with (albeit again much higher than) other work, such as the multi-model ensemble mean (MME) from PlioMIP2 models where increases rarely exceed ~1.2 mm day^{-1} (H20; see Section 4.2). These changes, and indeed the temperature changes over Northern Hemisphere landmasses, may be associated with changes to the total cloud cover, shown in Figure 10. Although the changes are small at the annual timescale (Fig. 10a), during Northern Hemisphere winter (Fig. 10b) there is a noticeable increase in cloud cover (of ~10%) over high latitude regions, corresponding to the increases in precipitation. Likewise, during Northern Hemisphere summer (Fig. 10c) there is a large reduction (over 20% in places) in cloud cover, especially over Northern Hemisphere landmasses; these regions, such as Europe and Northern Asia, correspond well to the areas of decreased precipitation and increased temperature.

https://doi.org/10.5194/cp-2021-40
Preprint. Discussion started: 21 April 2021

Climate of the Past Discussions
Open Access
EGU

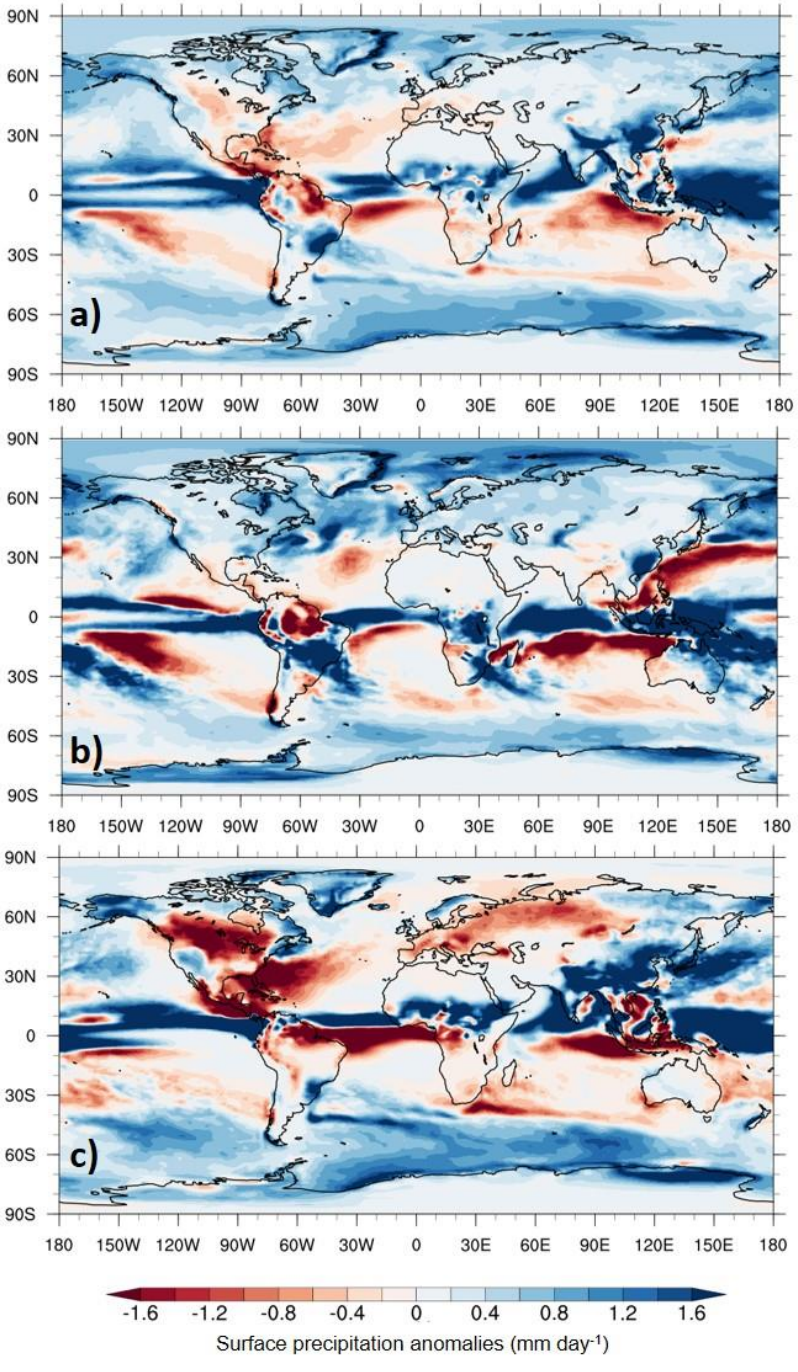

Figure 9 – Surface precipitation climatology differences (*mPWP – piControl_mod*) from HadGEM3. a) Annual; b) DJF; c) JJA

https://doi.org/10.5194/cp-2021-40
Preprint. Discussion started: 21 April 2021

Climate of the Past Discussions
Open Access
EGU

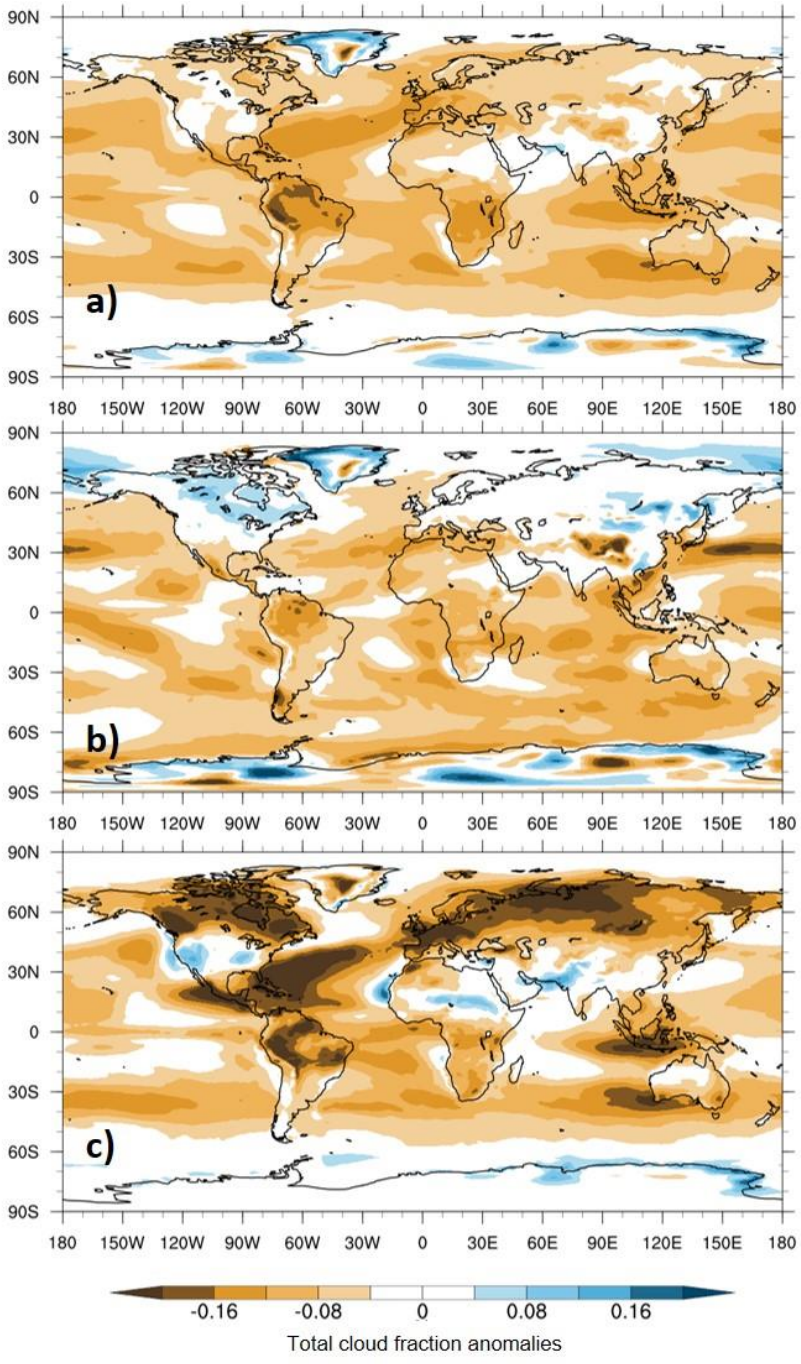

Figure 10 – Total cloud fraction climatology differences (*mPWP – piControl_mod*) from HadGEM3. a) Annual; b) DJF; c) JJA

https://doi.org/10.5194/cp-2021-40
Preprint. Discussion started: 21 April 2021

Climate of the Past Discussions
Open Access
EGU

4. COMPARISON OF HADGEM3 WITH OTHER MODELS AND PROXY DATA

4.1. Model-model and model-data comparison: Different generations of UK model versus proxy data

Here the focus is on mean SST differences between different generations of the UK's physical climate model, starting with three Pliocene simulations using the original fully-coupled climate model HadCM3, then a simulation from the more recent HadGEM2 and finally the *mPWP* simulation from HadGEM3. See Supplementary Material for details of these older models. For HadCM3, three separate Pliocene simulations (and corresponding PIs) are used; the first two were conducted by Lunt *et al*. (2011) and Bragg *et al*. (2012), and are referred to as HadCM3-PRISM2 and HadCM3-PlioMIP1, respectively (see Table 2). This is to distinguish them from a third version of the same model included in PlioMIP2, referred to here as HadCM3-PlioMIP2.

Model	Model name here	MIP	Boundary conditions	Reference
HadCM3	HadCM3-PRISM2	-	PRISM2	Lunt *et al*. 2011
HadCM3	HadCM3-PlioMIP1	PlioMIP1	PRISM3	Bragg *et al*. 2012
HadCM3	HadCM3-PlioMIP2	PlioMIP2	PRISM4	Hunter *et al*. 2019
HadGEM2-AO	HadGEM2	PlioMIP1	PRISM3	Tindall and Haywood 2020
HadGEM3-GC31-LL	HadGEM3	PlioMIP2	PRISM4	Presented here

Table 2 - Different generations of the UK physical climate model used here, and their involvement with PlioMIP

For comparative purposes, multi-proxy SST data from the KM5c interglacial, compiled by McClymont *et al*. (2020), were used. Here, they focus on a narrow time-slice from 3.195 to 3.215 Ma, and compile the SST data from two proxies: an alkenone-derived $U^{K'}_{37}$ index (Prahl and Wakeham, 1987) and foraminifera calcite Mg/Ca (Delaney *et al*. 1985), with the resulting data comprising the PlioVAR synthesis and covering 32 locations between 46°S-69°N (McClymont *et al*. 2020). See Data Availability for access details.

Maps of annual mean SST anomalies from the simulations, overlaid with the proxy data, are shown in Figure 11 and summary statistics are shown in Table 3.

https://doi.org/10.5194/cp-2021-40
Preprint. Discussion started: 21 April 2021

Climate of the Past Discussions
Open Access
EGU

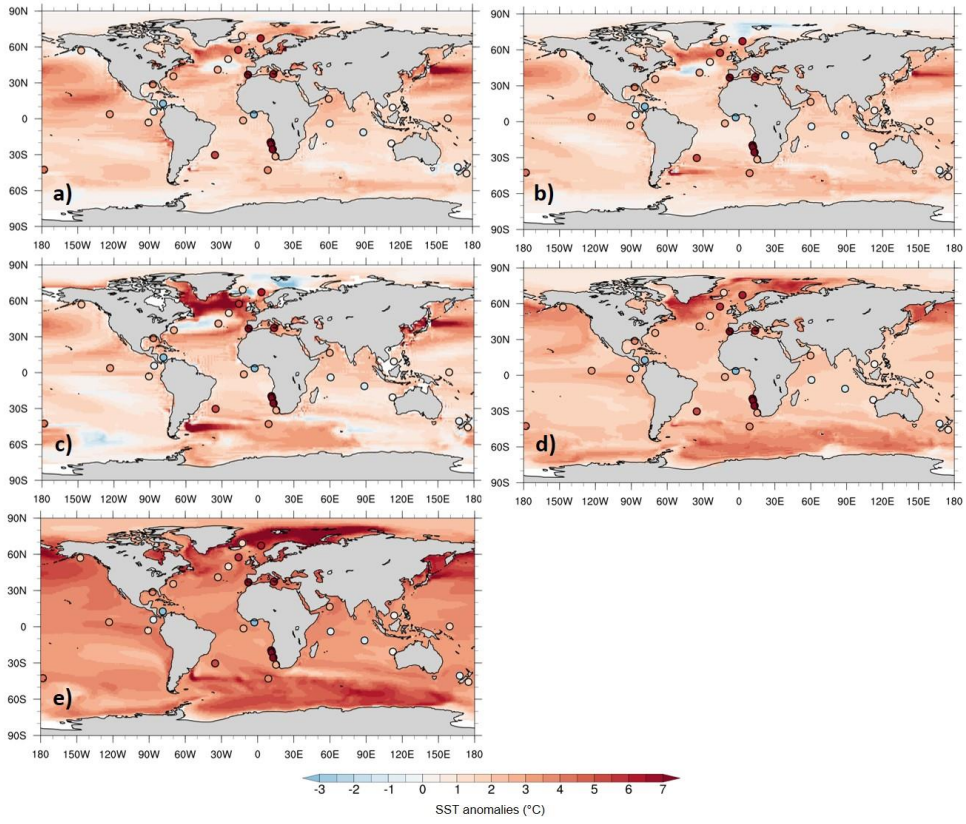

Figure 11 – SST climatology differences (Pliocene – PI) from different generations of the UK's physical climate model. a) HadCM3-PRISM2; b) HadCM3-PlioMIP1; c) HadCM3-PlioMIP2; d) HadGEM2; e) HadGEM3. Background gridded data shows model simulations, filled circles show SST proxy data from McClymont *et al*. (2020)

	HadCM3-PRISM2	HadCM3-PlioMIP1	HadCM3-PlioMIP2	HadGEM2	HadGEM3
Global mean (°C)	1.63	1.53	1.67	2.29	3.80
RMSE	3.55	3.62	3.59	3.23	3.36

Table 3 - Global annual mean SST anomalies from Pliocene simulations using different generations of the UK's physical climate model, and RMSE values between simulations and SST proxy data from McClymont *et al*. (2020)

https://doi.org/10.5194/cp-2021-40
Preprint. Discussion started: 21 April 2021


Climate of the Past Discussions

538 The global annual SST anomaly for HadGEM3 is 3.8°C, followed by HadGEM2 at 2.3°C, and then
539 1.7°C, 1.5°C and 1.6°C for the three HadCM3 simulations (starting with the most recent, HadCM3-
540 PlioMIP2; see Table 3). Comparing the newest model (HadGEM3) with the oldest model (HadCM3-
541 PRISM2), which have an anomaly of 3.8°C and 1.6°C respectively, clearly the most recent generation
542 is showing a much warmer Pliocene.
543
544 Comparing an earlier generation of the model with a later generation (HadCM3-PlioMIP1 and
545 HadGEM2, respectively; Fig. 11b and Fig. 11d), aside from the greater overall warming (2.3°C in
546 HadGEM2 versus 1.5°C in HadCM3-PlioMIP1) already discussed above, the main spatial patterns of
547 warming are similar, with both showing the greatest warming over the Labrador Sea and the north-
548 west Pacific and HadGEM2 showing greater polar amplification (PA) overall. In part thanks to this
549 high latitude warming, root mean squared error (RMSE) values are 3.2°C and 3.6°C for HadGEM2
550 and HadCM3-PlioMIP1, respectively, showing a greater agreement with the proxy data from
551 HadGEM2 (Table 3).
552
553 Likewise, comparing the other older model with the most recent (HadCM3-PlioMIP2 and HadGEM3,
554 respectively; Fig. 11c and Fig. 11e), the spatial patterns of warming differ more widely, with
555 HadGEM3 showing widespread Northern Hemisphere high latitude warming that is not shown by
556 HadCM3-PlioMIP2 at all, other than in the Labrador Sea. HadGEM3, and indeed HadGEM2, are
557 displaying a greater extent of PA in both hemispheres (Fig. 11d-e). As the warmest model,
558 HadGEM3 (RMSE = 3.4°C) is showing less agreement with the proxy data than HadGEM2 (RMSE =
559 3.2°C), likely because it is so warm that the discrepancy with the colder proxy data locations (such as
560 in the Indian Ocean, near New Zealand or off equatorial Africa) is greater (Fig. 11e). This is in spite
561 of the fact that, in the warmer proxy data locations (such as in the North Atlantic and Arctic)
562 HadGEM3 is closer to the proxy data. In these regions, the earlier versions of the model (Fig. 11a-c)
563 are not even capturing the sign of change and are showing a weak cooling, in stark contrast to the
564 proxy data, that neither HadGEM2 nor HadGEM3 display (Fig. 11d-e). Where proxy data suggest
565 colder conditions, again none of the models are capturing the sign of change and all show widespread
566 warming, and this is most evident in HadGEM3 because of its particularly strong warming. The fact
567 that all of the HadCM3 simulations are showing several regions of cooling and have a higher RMSE
568 than the most recent versions suggests that this early model might be too cold. In contrast, the fact
569 that HadGEM3 has a higher RMSE than HadGEM2 suggests that, despite involving significant model
570 development (see Williams *et al*. 2020 for a summary), concerning Pliocene climate HadGEM3 may
571 actually be too warm. Therefore, whilst model development appears to have improved the model's
572 agreement with proxy data since earlier versions of the model, this only appears to be true up to a
573 certain point; the "sweet spot" appears to be HadGEM2.
574

https://doi.org/10.5194/cp-2021-40
Preprint. Discussion started: 21 April 2021

Climate of the Past Discussions
Open Access
EGU

575 **4.2. Model-model comparison: HadGEM3 versus PlioMIP2 models**

576 Finally, the focus here is on mean differences, again considering SAT and precipitation anomalies,
577 between the *mPWP* simulation from HadGEM3 and the Pliocene simulations from all other available
578 models included in PlioMIP2 (Table 4).

Model, and modelling centre responsible for simulation	Spatial resolution (lon x lat)	
	Atmosphere	Ocean
CCSM4, National Centre for Atmospheric Research, US	1° x 1°	1° x 1°
CCSM4_Utr, Utrecht University, the Netherlands	2.5° x 1.9°	1° x 1°
CCSM4_UoT, University of Toronto, Canada	1° x 1°	1° x 1°
CESM1.2, National Centre for Atmospheric Research, US	1° x 1°	1° x 1°
CESM2, National Centre for Atmospheric Research, US	1° x 1°	1° x 1°
COSMOS, Alfred Wagner Institute, Germany	3.75° x 3.75°	3.0° x 1.8°
EC-Earth3.3, Stockholm University, Sweden	1.125° x 1.125°	1° x 1°
GISS-E2-1-G, Goddard Institute for Space Studies, US	2.0° x 2.5°	1.0° x 1.25°
HadCM3, University of Leeds, UK	2.5° x 3.75°	1.25° x 1.25°
IPSLCM5A, Laboratoire des Sciences du Climat et de l'Environnement, France	3.75° x 1.9°	2.0° x 2.0°
IPSLCM5A2, Laboratoire des Sciences du Climat et de l'Environnement, France	3.75° x 1.9°	2.0° x 2.0°
IPSL-CM6A-LR, Laboratoire des Sciences du Climat et de l'Environnement, France	2.5° x 1.26°	1.0° x 1.0°
MIROC4m, University of Tokyo, Japan	2.8° x 2.8°	1.4° x 1.4°
MRI-CGCM2.3, University of Tsukuba, Japan	2.8° x 2.8°	2.0° x 2.0°
NorESM-L, Bjerknes Centre for Climate Research, Norway	3.75° x 3.75°	3.0° x 3.0°
NorESM-F, Bjerknes Centre for Climate Research, Norway	1.9° x 2.5°	1.0° x 1.0°

579
580 Table 4 - Climate models included here from PlioMIP2 (see Haywood *et al*. 2020 for each model's reference)
581
582
583
584
585

https://doi.org/10.5194/cp-2021-40
Preprint. Discussion started: 21 April 2021

Climate of the Past Discussions
Open Access
EGU

A number of different metrics of SAT are shown in Figure 12 for each of the models, as well as the MME; the panels shown here are updated versions of those shown in H20, but now including HadGEM3. It should be noted that, consistent with H20, the models are listed according to their published ECS, with the highest ECS listed first. HadGEM3 has an ECS of 5.5 K (Andrews *et al*. 2019), compared to the 2nd highest model (CESM2) with an ECS of 5.3 K (H20). If, however, all available models within CMIP6 (i.e. not just those having conducted Pliocene simulations) are considered, then HadGEM3 has the 2nd highest ECS, just below that of CanESM5 with an ECS of 5.6 K (Zelinka *et al*. 2020).

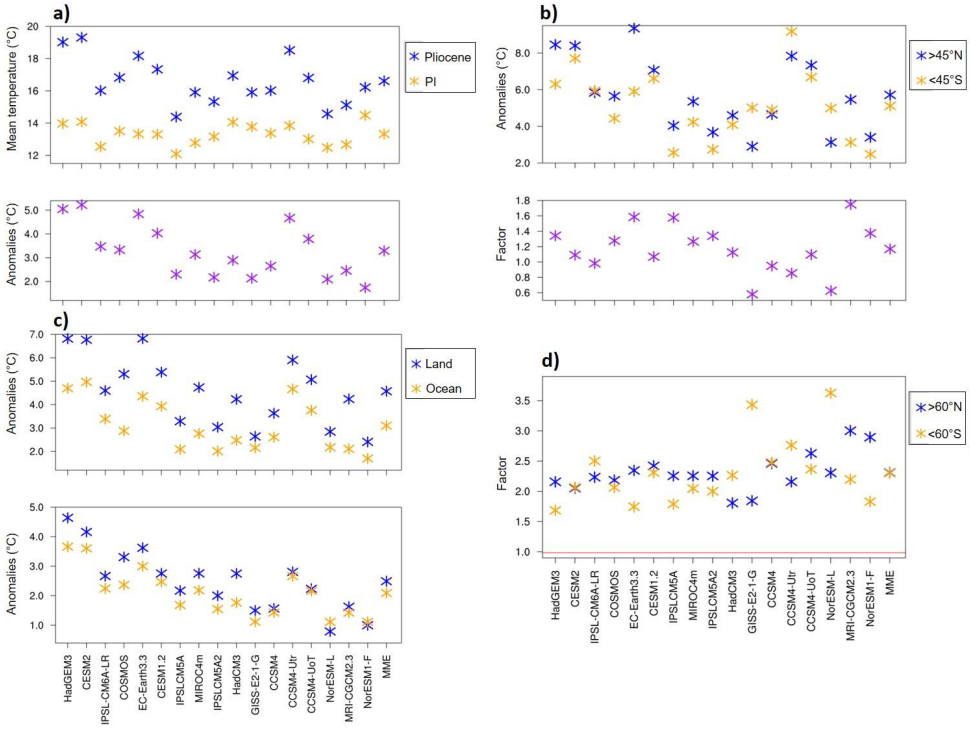

Figure 12 - SAT from Pliocene simulations from HadGEM3 and all other models in PlioMIP2. a) Global annual mean SAT (top panel) and anomalies (bottom panel); b) Extratropical (+/- 45°) annual mean SAT anomalies (top panel) and ratio (i.e. >45°N divided by <45°S) between them (bottom panel); c) Land and ocean annual mean SAT anomalies, averaged globally (top panel) and between 20°N-20°S (bottom panel); d) Annual mean SAT polar amplification i.e. SAT poleward of 60° divided by global mean, for each hemisphere, where red line = ratio of 1 (i.e. no polar amplification). Figures reproduced and adapted from Haywood *et al*. (2020)

As mentioned above (Section 3.2), the global annual SAT anomaly by the end of the *mPWP* simulation is 5.1°C, making HadGEM3 one of the warmest models in PlioMIP2 and second only to CESM2 (H20). This is true both in terms of its anomaly and its mean Pliocene SAT (19°C); this is only lagging behind the warmest model by 0.2°C and 0.3°C for the anomalous and mean SAT,

https://doi.org/10.5194/cp-2021-40
Preprint. Discussion started: 21 April 2021


Climate of the Past Discussions

606 respectively (Fig. 12a). HadGEM3 is much warmer than earlier global annual mean temperature
607 estimates (e.g. Haywood and Valdes 2004) and the range given by models included in PlioMIP1
608 (1.8°C to 3.6°C, see Haywood *et al*. (2013), and is at the top end of the range given by models
609 included in PlioMIP2 (1.7°C to 5.2°C, see H20). The impact of including HadGEM3 amongst the
610 models is to increase the MME anomaly by 0.1°C, from 3.2° to 3.3°C. Interestingly the HadGEM3
611 *piControl_mod* simulation is not presenting the warmest PI anomalies compared to the other models,
612 coming 4th in the list, suggesting that HadGEM3 is more sensitive to the Pliocene boundary conditions
613 rather than being a generally warmer model overall.
614
615 Concerning annual global mean precipitation (Fig. 13, top panel), as mentioned above the
616 precipitation anomaly by the end of the simulation is 0.34 mm day^{-1}, making HadGEM3 not only one
617 of the warmest models in PlioMIP2 but also one of the wettest (consistent with current understanding,
618 as global precipitation is generally a function of global temperature). The range of anomalies across
619 all models during PlioMIP1 was 0.09 to 0.18 mm day^{-1} (Haywood *et al*. 2013), during PlioMIP2 it
620 was 0.07 to 0.37 mm day^{-1} (with the higher values being attributed to the models being more sensitive
621 to the updated PRISM4 boundary conditions) and the PlioMIP2 ensemble mean was 0.19 mm day^{-1}
622 (H20). Concerning the mean, it is the wettest model in terms of both its *mPWP* (3.49 mm day^{-1}) and
623 *piControl_mod* (3.15 mm day^{-1}) simulations, and both of these are much higher than the MME (3.06
624 mm day^{-1} and 2.86 mm day^{-1} for the Pliocene and PI simulations, respectively). The fact that both the
625 HadGEM3 *mPWP* and *piControl_mod* simulations are not only the wettest, but are also closer
626 together in terms of mean precipitation, means that if the anomaly is considered (Fig. 13, bottom
627 panel) HadGEM3 is not quite the wettest model; an anomaly of 0.34 mm day^{-1} makes it 2nd only to
628 CCSM4-Utr (at 0.37 mm day^{-1}). The impact of including HadGEM3 amongst the other PlioMIP2
629 models is to again slightly increase the MME anomaly, from 0.19 mm day^{-1} as reported by H20 to 0.2
630 mm day^{-1} here.

https://doi.org/10.5194/cp-2021-40
Preprint. Discussion started: 21 April 2021

Climate of the Past Discussions

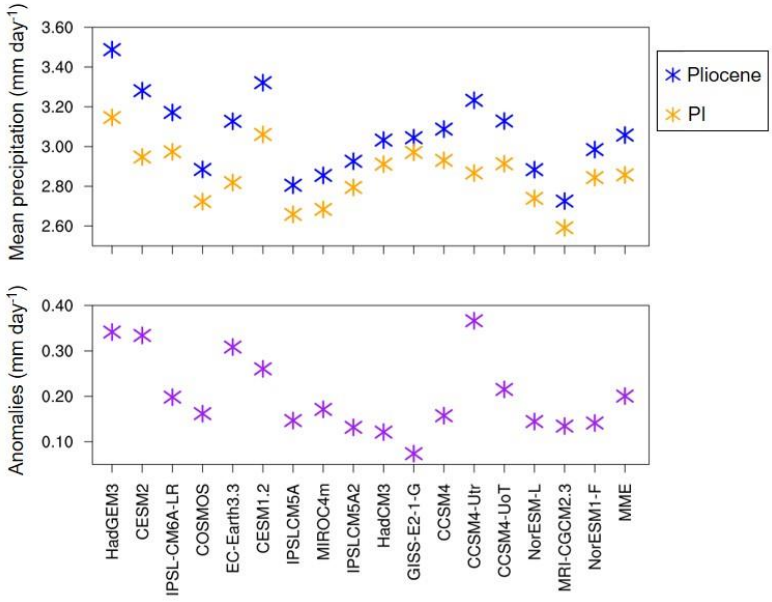

Figure 13 - Global annual mean surface precipitation (top panel) and anomalies (bottom panel) from HadGEM3 *mPWP* simulation and all other models in PlioMIP2, as well as multi-model ensemble mean (MME). Figure reproduced and adapted from Haywood *et al*. (2020)

Returning to SAT and if only extratropical warming (separated by hemisphere, above or below 45°N or S) is considered, then HadGEM3 agrees with the other 11 models (out of 16) that H20 identified as showing enhanced Northern Hemisphere warming, relative to the Southern Hemisphere (Fig. 12b, top panel). In the Northern Hemisphere, HadGEM3 is again one of the warmest models and, at 8.46°C, is considerably warmer than most other models and the MME; this, with the inclusion of HadGEM3, has now increased from the 5.5°C reported in H20 to 5.7°C here. However, in the Southern Hemisphere HadGEM3 is closer to many of the other models, albeit still in the top 33% of them, and with a warming of 6.3°C is much closer to the MME of 5.1°C (Fig. 12b, top panel). This is further demonstrated by Fig. 12b (bottom panel), showing the ratio of warming between the hemispheres (calculated by dividing the Northern Hemisphere warming by the Southern Hemisphere warming), where HadGEM3 is giving a ratio of 1.34 which is again close to many of the other models and the MME (1.17). Considering land-sea temperature contrasts (Fig. 12c), as H20 state all of the PlioMIP2 models show more warming over land, both globally and across the tropics (defined as 20°N-20°S), and HadGEM3 is no exception. Indeed, over either land or sea, HadGEM3 is the 2nd warmest globally and warmest across the tropics, and the inclusion of this model increases the MME by 0.1-0.14°C depending on whether land or sea warming is considered.

https://doi.org/10.5194/cp-2021-40
Preprint. Discussion started: 21 April 2021


Climate of the Past Discussions
Open Access
EGU

653 In contrast to the above metrics, where HadGEM3 is one of the largest outliers regardless of metric,
654 concerning polar amplification (PA) this is not the case. Here, as in H20, PA is defined as the ratio of
655 SAT increases poleward of 60° divided by the global mean SAT increases (Smith *et al*. 2019),
656 calculated independently for each hemisphere. Despite the HadGEM3 *mPWP* simulation qualitatively
657 showing considerable PA at both annual and seasonal timescales (Figure 7), when quantitatively
658 compared with all other PlioMIP2 models HadGEM3 is, whilst still having PA >1 (i.e. that there is
659 some amplification of warming around the poles), nevertheless showing considerably less PA in both
660 hemispheres, and is also lower than the MME in both hemispheres (Fig. 12d). Of all the models,
661 HadGEM3 comes 4th-to-last for Northern Hemisphere PA and last for Southern Hemisphere PA, and
662 its inclusion with the other models reduces the MME ratio by approximately 0.01 and 0.04 for the
663 Northern and Southern Hemisphere, respectively. This is consistent with the conclusions of H20, who
664 note a weak relationship between ECS and PA; they observe that models with a lower ECS tend to
665 display higher PA, and therefore the converse appears to be true here i.e. HadGEM3, with one of the
666 highest ECS, is displaying one of the lowest amounts of PA. The PA for all the models, as well as the
667 MME, can be seen graphically in Figure S9 in the Supplementary Material where, at first glance,
668 HadGEM3 would appear to be showing one of the largest amounts of PA. However, and consistent
669 with the observation by H20, the relatively low PA in HadGEM3 is not because the model is showing
670 less warming at high latitudes but rather because it is showing more warming in the tropics, compared
671 to the other models.
672
673 Lastly, concerning SST anomalies the HadGEM3 *mPWP* simulation is warmer than most other
674 models in PlioMIP2 (Figure 14). When simulated SST is compared to the proxy data from
675 McClymont *et al*. (2020), if the models are ranked according to RMSE then the HadGEM3 *mPWP*
676 simulation (RMSE = 3.4°C) ranks approximately halfway amongst them, suggesting better agreement
677 with the proxy data relative to some of the much cooler models (e.g. NorESM1-F, where RMSE =
678 3.9°C). There appears to be a weak relationship between the warmth of the model and agreement
679 with proxy data, with some of the other warm models (e.g. CESM2, the warmest model) showing less
680 agreement (RMSE = 3.5°C) with the proxy data than HadGEM3; however, this is not always true,
681 such as the case of the CCSM4-Utr which is also comparatively warm but is showing a slightly better
682 agreement (RMSE = 3.3°C) with the proxy data. It is likely that the location of the proxy data is
683 important, as the best agreement comes from the MME (RMSE = 3.1°C) which is showing warm SST
684 anomalies over the North Atlantic and Arctic (better in agreement with the proxy data there) but less
685 warming relative to HadGEM3 and CESM2 in the Southern Hemisphere (better in agreement with the
686 proxy data in e.g. the Indian Ocean).

https://doi.org/10.5194/cp-2021-40
Preprint. Discussion started: 21 April 2021

Climate of the Past Discussions
Open Access
EGU

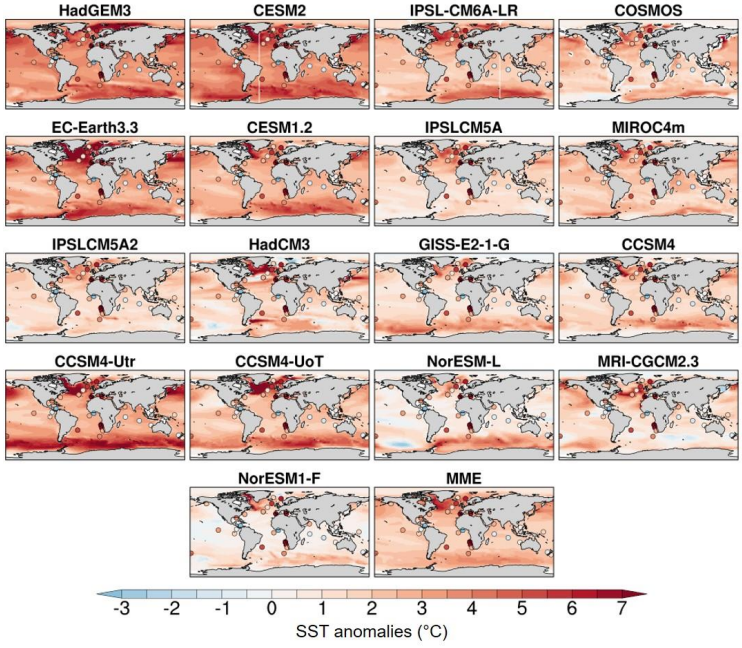

	RMSE (°C)
HadGEM3	3.4
CESM2	3.5
IPSL-CM6A-LR	3.1
COSMOS	3.3
EC-Earth3.3	3.6
CESM1.2	3.1
IPSLCM5A	3.2
MIROC4m	3.5
IPSLCM5A2	3.4
GISS-E2-1-G	3.5
CCSM4	3.3
CCSM4-Utr	3.3
CCSM4-UoT	3.3
NorESM-L	3.1
MRI-CGCM2.3	3.5
NorESM1-F	3.9
MMM	3.1

Figure 14 – SST climatology differences (Pliocene – PI) from HadGEM3 *mPWP* simulation and all other models in PlioMIP2, as well as multi-model ensemble mean (MME). Table shows RMSE scores when compared proxy data from McClymont *et al.* (2020)

5. SUMMARY AND CONCLUSIONS

This study has introduced the mid-Pliocene simulation using the latest version of the UK's physical climate model, HadGEM3-GC31-LL, presented the experimental design and conducted a model-model and model-data comparison. This study is novel, being the first time this version of the UK model has been run this far back in time; only two other paleoclimate simulations using this model have thus far been conducted, comprising the UK's contribution to CMIP6/PMIP4, and both of these were more recent, Quaternary simulations (Williams *et al.* 2020).

The *mPWP* simulation mostly followed the experimental design defined in H16, with the exception being the exclusion of a Pliocene LSM and Pliocene soils. Both of these were kept the same as PI. All other boundary conditions, including CO_2, orography, ice mask, lakes, vegetation fractions and vegetation functional types followed the protocol of H16, and were incrementally implemented to be Pliocene, based on the PRISM4 dataset. A minor model parameter change was included to increase the model's stability in light of the strong Pliocene forcing, and thus a corresponding PI simulation was also run for comparison purposes The *mPWP* simulation was run for 567 years in total, during which atmospheric and oceanic equilibrium were assessed. Although not meeting the criteria used to determine equilibrium in other paleoclimate simulations, especially concerning oceanic equilibrium,

https://doi.org/10.5194/cp-2021-40
Preprint. Discussion started: 21 April 2021


Climate of the Past Discussions

709 due to computational restrictions it was not possible to run this model for the thousands of years
710 required to achieve this.
711
712 The results presented here are divided into three sections: i) a simulation comparison, in which the
713 *mPWP* simulation is compared to its corresponding *piControl_mod* simulation (Section 3.2); ii) a
714 model-model and model-data comparison, in which the most recent *mPWP* simulation is compared to
715 Pliocene simulations from previous versions of the same model, all assessed against proxy data
716 (Section 4.1); and iii) a model-model comparison, in which the most recent *mPWP* simulation is
717 compared to other models (Section 4.2).
718
719 For the first comparison, the *mPWP* simulation is behaving in line with current understanding and
720 previous work (e.g. Haywood *et al*. 2013, H20), showing a warmer and wetter world relative to the PI,
721 with the greatest warming occurring over the poles. This polar warming, which can be attributed to a
722 loss in sea ice and changes in clouds, and the changes to precipitation (such as an enhancement of
723 monsoon systems) all agree with the expected response and previous work (e.g. Cronin *et al*. 1993,
724 Howell *et al*. 2016, Li *et al*. 2018, Moran *et al*. 2006, Polyak *et al*. 2010, Zhang *et al*. 2013, 2016).
725 For the second comparison, there is a clear increase in global temperatures (as measured by SST) as
726 the model develops through time, beginning with the early Pliocene simulations using HadCM3 (Lunt
727 *et al*. 2011 and Bragg *et al*. 2012), through HadGEM2 (Tindall and Haywood 2020) and up to the
728 most recent *mPWP* simulation from HadGEM3, presented here. Up to a point, this warming results in
729 a better agreement with available proxy data. However, just as the earlier HadCM3 simulations
730 appear to be too cold relative to some proxy data, the most recent *mPWP* simulation from HadGEM3
731 appears to be too warm; the "sweet spot" appears to be the previous generation of the model,
732 HadGEM2. For the third comparison, the above conclusion that HadGEM3 is too warm is further
733 suggested by the fact that it is one of the warmest and wettest models in all of PlioMIP2 (H20), and
734 this is true over either land or sea and especially in the Northern Hemisphere. When compared to
735 proxy SST data, HadGEM2 ranks approximately halfway amongst the models, and is much too warm
736 in certain locations, such as the Indian Ocean. However, the conclusion that the model is too warm
737 overall is argued by the fact that the anomalies coming from the HadGEM3 *piControl_mod*
738 simulation are not the warmest, suggesting that rather than the model being too warm in general, the
739 excess warming may be coming from the model's sensitivity to the Pliocene forcing. This would be
740 consistent with the model's high ECS, which is among the highest (if not the highest) of all the most
741 recent state-of-the-art CMIP6 models (Andrews *et al*. 2019, H20, Zelinka *et al*. 2020). This high
742 sensitivity further it is suggested by the fact that the *mPWP* simulation is not yet in true equilibrium
743 by the time the climatologies are calculated, as shown by Figure 6 where there is clearly some
744 warming still to happen.
745

https://doi.org/10.5194/cp-2021-40
Preprint. Discussion started: 21 April 2021


Climate of the Past Discussions

A number of caveats should be mentioned in this study. Firstly, any differences to the PlioMIP2 models may be in part related to the fact that the LSM used here is identical to the *piControl*, rather than using the enhanced LSM following the experimental design of H16. This, as discussed above, was necessary, due to technical difficulties in coupling a new LSM to the atmosphere. One of the impacts of this is discussed in Zhang *et al*. (2021), who investigated Atlantic Meridional Overturning Circulation (AMOC) changes during the Pliocene using the PlioMIP2 models. It was found that in contrast to most other PlioMIP2 models, which stimulate a stronger AMOC in the Pliocene relative to the PI, HadGEM3 shows a weaker AMOC, with a maximum of 14.3 Sv and 16.1 Sv for the *mPWP* and *piControl_mod* simulations, respectively (Zhang *et al*. 2021). Secondly, using PI soil parameters and soil dust properties (away from ice regions) may also have an impact on the observed warming; although H16 does provide a set of palaeosol data from Pound *et al*. (2016), this was not used here because of the difficulties in matching the reconstructions to the model's soil-related fields. Thirdly, concerning greenhouse gas forcings, in all of the Pliocene simulations discussed here only CO_2 was modified, with other gases such as methane being left as PI. Given that these trace gases will likely amplify warming, especially in the extratopics (Hopcroft *et al*. 2020), leaving these as PI may be resulting in a cooler climate in all of the simulations. Lastly, excess warming in the *mPWP* simulation may be because certain processes, in particular vegetation, were fixed rather than being interactive (although this is also the case in the majority of the other PlioMIP2 models). In particular, the fact that the introduction of Pliocene vegetation in the *mPWP* simulation results in such a dramatic rise in global SAT (Figure 6) deserves much further exploration. This may be highly important regarding any possible climate sensitivity under a Pliocene-style forcing, and therefore current work is underway to investigate the role of vegetation in contributing to the model's simulated warming.

DATA AVAILABILITY

Selected fields, such as SAT, precipitation and SST, from the HadGEM3 *mPWP* simulation are currently available from the Earth System Grid Federation (ESGF) WCRP Coupled Model Intercomparison Project (Phase 6), located at https://esgf-node.llnl.gov/projects/cmip6/ (last access: 18 March 2021). If other fields are required, they can be made available to the public by directly contacting the lead author. Likewise, access to the other model simulations considered here can be gained by contacting the lead author, or the authors of the appropriate publication. For the SST reconstructions, the data can be found within the Supplementary Online Material of McClymont *et al*. (2020), available online at: https://doi.org/10.5194/cp-16-1599-2020-supplement.

AUTHOR CONTRIBUTIONS

CJRW conducted the *mPWP* simulation, carried out the analysis, produced some of the figures, wrote the majority of the manuscript, and led the paper. XR produced some of the figures. AAS, WHGR, RSS, PH and EJS provided technical assistance in running HadGEM3. JCT, SJH and AMH also

https://doi.org/10.5194/cp-2021-40
Preprint. Discussion started: 21 April 2021


Climate of the Past Discussions

783 provided technical assistance, and contributed the HadGEM2 and HadCM3 simulations. DJL
784 contributed to some of the writing. All authors proofread the paper and provided comments.
785
786 **COMPETING INTERESTS**
787 The authors declare that they have no conflict of interest.
788
789 **ACKNOWLEDGEMENTS**
790 CJRW and DJL acknowledge the financial support of the UK Natural Environment Research Council
791 (NERC)-funded SWEET project, research grant NE/P01903X/1. AAS was supported by the Met
792 Office Hadley Centre Climate Programme, funded by BEIS and Defra. XR was supported by the 4D-
793 REEF project, receiving funding from the European Union's Horizon 2020 research and innovation
794 programme under the Marie Skłodowska-Curie research grant, no. 813360. PH was supported by a
795 University of Birmingham Fellowship. RSS was funded by the NERC national capability grant for
796 the UK Earth System Modelling (UKESM) project, research grant NE/N017951/1. AMH and JCT
797 acknowledge receipt of funding from the European Research Council under the European Union's
798 Seventh Framework Programme (FP7/2007-2013)/ERC, grant agreement no. 278636.
799
800 **FINANCIAL SUPPORT**
801 This research has been supported by the NERC-funded SWEET project (grant no. NE/P01903X/1),
802 the Met Office Hadley Centre Climate Programme (funded by BEIS and Defra), the European Union's
803 Horizon 2020 research and innovation programme under the Marie Skłodowska-Curie research grant
804 (no. 813360), a University of Birmingham Fellowship, the NERC UKESM project (grant no.
805 NE/N017951/1) and the European Union's Seventh Framework Programme (FP7/2007-2013)/ERC
806 (grant no. 278636).
807
808 **LIST OF TABLES**
809 Table 1 - Centennial trends (calculated via a linear regression) in global mean measures of climate
810 equilibrium over the last 50 years of the simulations, adapted from Menary *et al*. (2018) to include the
811 CMIP6 *piControl*, *piControl_mod* and *mPWP* simulations. Negative TOA radiation = net radiation
812 flux is downward
813
814 Table 2 - Different generations of the UK physical climate model used here, and their involvement
815 with PlioMIP
816
817 Table 3 - Global annual mean SST anomalies from Pliocene simulations using different generations of
818 the UK's physical climate model, and RMSE values between simulations and SST proxy data from
819 McClymont *et al*. (2020)

https://doi.org/10.5194/cp-2021-40
Preprint. Discussion started: 21 April 2021


Climate of the Past Discussions

Table 4 - Climate models included here from PlioMIP2 (see Haywood *et al*. 2020 for each model's reference)

LIST OF FIGURES

https://doi.org/10.5194/cp-2021-40
Preprint. Discussion started: 21 April 2021


Climate of the Past Discussions

Figure 7 – 1.5 m air temperature climatology differences (*mPWP* – *piControl_mod*) from HadGEM3. a) Annual; b) DJF; c) JJA

Figure 8 – Sea ice fraction climatology differences (*mPWP* – *piControl_mod*) from HadGEM3. a) Annual; b) DJF; c) JJA

Figure 9 – Surface precipitation climatology differences (*mPWP* – *piControl_mod*) from HadGEM3. a) Annual; b) DJF; c) JJA

Figure 10 – Total cloud fraction climatology differences (*mPWP* – *piControl_mod*) from HadGEM3. a) Annual; b) DJF; c) JJA

Figure 11 – SST climatology differences (Pliocene – PI) from different generations of the UK's physical climate model. a) HadCM3-PRISM2; b) HadCM3-PlioMIP2; c) HadCM3-PlioMIP2; d) HadGEM2; e) HadGEM3. Background gridded data shows model simulations, filled circles show SST proxy data from McClymont *et al*. (2020)

Figure 12 - SAT from Pliocene simulations from HadGEM3 and all other models in PlioMIP2. a) Global annual mean SAT (top panel) and anomalies (bottom panel); b) Extratropical (+/- 45°) annual mean SAT anomalies (top panel) and ratio (i.e. >45°N divided by <45°S) between them (bottom panel); c) Land and ocean annual mean SAT anomalies, averaged globally (top panel) and between 20°N-20°S (bottom panel); d) Annual mean SAT polar amplification i.e. SAT poleward of 60° divided by global mean, for each hemisphere, where red line = ratio of 1 (i.e. no polar amplification). Figures reproduced and adapted from Haywood *et al*. (2020)

Figure 13 - Global annual mean surface precipitation (top panel) and anomalies (bottom panel) from HadGEM3 *mPWP* simulation and all other models in PlioMIP2, as well as multi-model ensemble mean (MME). Figure reproduced and adapted from Haywood *et al*. (2020)

Figure 14 – SST climatology differences (Pliocene – PI) from HadGEM3 *mPWP* simulation and all other models in PlioMIP2, as well as multi-model ensemble mean (MME). Table shows RMSE scores when compared proxy data from McClymont *et al*. (2020)

https://doi.org/10.5194/cp-2021-40
Preprint. Discussion started: 21 April 2021

Climate of the Past Discussions

REFERENCES

Andrews, T., Andrews, M. B., Bodas-Salcedo, A., Jones, G. S., Kuhlbrodt, T., Manners, J., Menary, M. B., Ridley, J., Ringer, M. A., Sellar, A. A., Senior, C. A. and Tang, Y.: Forcings, feedbacks, and climate sensitivity in HadGEM3-GC3.1 and UKESM1, JAMES, https://doi.org/10.1029/2019MS001866, 2019.

Best, M. J., Pryor, M., Clark, D. B., Rooney, G. G., Essery, R. L. H., Ménard, C. B., Edwards, J. M., Hendry, M. A., Gedney, N., Mercado, L. M., Sitch, S., Blyth, E., Boucher, O., Cox, P. M., Grimmond, C. S. B. And Harding, R. J.: The Joint UK Land Environment Simulator (JULES), model description – Part 1: Energy and water fluxes, Geosci. Model Dev., 4, 677–699, https://doi.org/10.5194/gmd-4-677-2011, 2011.

Berntell, E., Zhang, Q., Li, Q., Haywood, A. M., Tindall, J. C., Hunter, S. J., Zhang, Z., Li, X., Guo, C., Nisancioglu, K. H., Stepanek, C., Lohmann, G., Sohl, L. E., Chandler, M. A., Tan, N., Contoux, C., Ramstein, G., Baatsen, M. L. J., von der Heydt, A. S., Chandan, D., Peltier, W. R., Abe-Ouchi, A., Chan, W.-L., Kamae, Y., Williams, C. J. R. and Lunt, D. J.: Mid-Pliocene West African Monsoon Rainfall as simulated in the PlioMIP2 ensemble, Clim. Past Discuss. [preprint], https://doi.org/10.5194/cp-2021-16, in review, 2021.

Bragg, F. J., Lunt, D. J. and Haywood, A. M.: Mid-Pliocene climate modelled using the UK Hadley Centre Model: PlioMIP Experiments 1 and 2, Geosci. Model Dev., 5, 1109-1125, doi:10.5194/gmd-5-1109-2012, 2012.

Burke, K. D., Williams, J. W., Chandler, M. A., Haywood, A. M., Lunt, D. J. and Otto-Bliesner, B. L.: Pliocene and Eocene provide best analogs for near-future climates, PNAS, 115, 13288-13293, 10.1073/pnas.1809600115, 2018

Clark, D. B., Mercado, L. M., Sitch, S., Jones, C. D., Gedney, N., Best, M. J., Pryor, M., Rooney, G. G., Essery, R. L. H., Blyth, E., Boucher, O., Cox, P. M., and Harding, R. J.: The Joint UK Land Environment Simulator (JULES), model description – Part 2: Carbon fluxes and vegetation, Geosci. Model Dev., 4, 701–722, https://doi.org/10.5194/gmd-4-701-2011, 2011.

Cronin, T. M., Whatley, R. C.,Wood, A., Tsukagoshi, A., Ikeya, N., Brouwers, E. M., and Briggs, W. M.: Microfaunal evidence for elevated mid-Pliocene temperatures in the Arctic Ocean, Paleoceanography, 8, 161-173, https://doi.org/10.1029/93PA00060, 1993.

https://doi.org/10.5194/cp-2021-40
Preprint. Discussion started: 21 April 2021

928 Crucifix, M., Betts R. A. and Hewitt, C. D.: Pre-industrial-potential and Last Glacial Maximum global
929 vegetation simulated with a coupled climate-biosphere model: Diagnosis of bioclimatic relationships,
930 Glob. Planet. Chang, 45 (4), 295-312, DOI: 10.1016/j.gloplacha.2004.10.001, 2005.
931
932 Collins, W. J., Bellouin, N., Doutriaux-Boucher, M., Gedney, N., Halloran, P., Hinton, T., Hughes, J.,
933 Jones, C. D., Joshi, M., Liddicoat, S., Martin, G., O'Connor, F., Rae, J., Senior, C., Sitch, S.,
934 Totterdell, I., Wiltshire, A., Woodward, S.: Development and evaluation of an Earth-System model-
935 HadGEM2. Geosci. Model Dev. 4, 1051–1075. https://doi.org/10.5194/gmd-4-1051-2011, 2011.
936
937 Cox, P. M.: Description of the TRIFFID Dynamic Global Vegetation Model - Hadley Centre
938 Technical Note 24, Met Office, Bracknell, https://jules.jchmr.org/sites/default/files/HCTN_24.pdf,
939 2001.
940
941 Cox, P. M., Betts, R. A., Bunton, C. B., Essery, R. L. H., Rowntree, PR. and Smith, J.: The impact of
942 new land surface physics on the GCM simulation of climate and climate sensitivity, Clim. Dyn., 15,
943 183-203, https://doi.org/10.1007/s003820050276, 1999.
944
945 Delaney, M. L., Be, A. W. H., and Boyle, E. A.: Li, Sr, Mg, and Na in foraminiferal calcite shells
946 from laboratory culture, sediment traps, and sediment cores, Geochim. Cosmochim. Ac., 49, 1327-
947 1341, 1985.
948
949 Dowsett, H. J.: The PRISM palaeoclimate reconstruction and Pliocene sea-surface temperature, in:
950 Deep-Time Perspectives on Climate Change: Marrying the Signal from Computer Models and
951 Biological Proxies, edited by: Williams, M., Haywood, A. M., Gregory, F. J., and Schmidt, D. N.,
952 Bath, UK, Geological Soc Publishing House, 459-480, 2007.
953
954 Dowsett, H. J., Robinson, M., Haywood, A., Salzmann, U., Hill, D., Sohl, L., Chandler, M., Williams,
955 M., Foley, K., and Stoll, D.: The PRISM3D paleoenvironmental reconstruction, Stratigraphy, 7, 123-
956 139, 2010.
957
958 Dowsett, H., Dolan, A., Rowley, D., Moucha, R., Forte, A. M., Mitrovica, J. X., Pound, M.,
959 Salzmann, U., Robinson, M., Chandler, M., Foley, K., and Haywood, A.: The PRISM4 (mid-
960 Piacenzian) paleoenvironmental reconstruction, Clim. Past, 12, 1519-1538,
961 https://doi.org/10.5194/cp-12-1519-2016, 2016.
962

https://doi.org/10.5194/cp-2021-40
Preprint. Discussion started: 21 April 2021


Climate of the Past Discussions

963 Essery, R. L. H., Best, M. J., Betts, R. A., Cox, P. M., and Taylor, C. M.: Explicit representation of
964 subgrid heterogeneity in a GCM land surface scheme, J. Hydrometeor., 4, 530–543,
965 https://doi.org/10.1175/1525-7541(2003)004<0530:EROSHI>2.0.CO;2, 2003.
966
967 Essery, R. L. H., Best, M. J. and Cox, P. M.: MOSES 2.2 Technical Documentation - Hadley Centre
968 Technical Note 30, Met Office, Bracknell. https://jules.jchmr.org/sites/default/files/HCTN_30.pdf,
969 2001.
970
971 Foley, K. M. and Dowsett, H. J.: Community sourced mid-Piacenzian sea surface temperature (SST)
972 data, US Geological Survey data release, https://doi.org/10.5066/P9YP3DTV, 2019.
973
974 Gordon, C., Cooper, C., Senior, C. A., Banks, H., Gregory, J. M., Johns, T. C., Mitchell, J. F. B., and
975 Wood, R. A.: The simulation of SST, sea ice extents and ocean heat transports in a version of the
976 Hadley Centre coupled model without flux adjustments, Clim. Dynam., 16, 147-168, 2000.
977
978 Hardiman, S. C., Andrews, M. B., Andrews, T., Bushell, A. C., Dunstone, N. J., Dyson, H., Jones, G.
979 S., Knight, J. R., Neininger, E., O'Connor, F. M., Ridley, J. K., Ringer, M. A., Scaife, A. A., Senior,
980 C. A. and Wood, R. A.: The impact of prescribed ozone in climate projections run with HadGEM3-
981 GC3.1, JAMES, 11, https://doi.org/10.1029/2019MS001714, 2019.
982
983 Harrison, S. P. and Prentice, I. C.: Climate and CO_2 controls on global vegetation distribution at the
984 last glacial maximum: analysis based on palaeovegetation data, biome modelling and palaeoclimate
985 simulations, Glob. Change Bio., 9 (7), 983-1004, https://doi.org/10.1046/j.1365-2486.2003.00640.x,
986 2003.
987
988 Haywood, A. M., Dowsett, H. J., Dolan, A. M., Rowley, D., Abe-Ouchi, A., Otto-Bliesner, B.,
989 Chandler, M. A., Hunter, S. J., Lunt, D. J., Pound, M., and Salzmann, U.: The Pliocene Model
990 Intercomparison Project (PlioMIP) Phase 2: scientific objectives and experimental design, Clim. Past,
991 12, 663–675, https://doi.org/10.5194/cp-12-663-2016, 2016
992
993 Haywood, A. M., Hill, D. J., Dolan, A. M., Otto-Bliesner, B. L., Bragg, F., Chan, W.-L., Chandler, M.
994 A., Contoux, C., Dowsett, H. J., Jost, A., Kamae, Y., Lohmann, G., Lunt, D. J., Abe-Ouchi, A.,
995 Pickering, S. J., Ramstein, G., Rosenbloom, N. A., Salzmann, U., Sohl, L., Stepanek, C., Ueda, H.,
996 Yan, Q., and Zhang, Z.: Large-scale features of Pliocene climate: results from the Pliocene Model
997 Intercomparison Project, Clim. Past, 9, 191-209, https://doi.org/10.5194/cp-9-191-2013, 2013
998

https://doi.org/10.5194/cp-2021-40
Preprint. Discussion started: 21 April 2021

999 Haywood, A. M., Tindall, J. C., Dowsett, H. J., Dolan, A. M., Foley, K. M., Hunter, S. J., Hill, D. J.,
1000 Chan, W.-L., Abe-Ouchi, A., Stepanek, C., Lohmann, G., Chandan, D., Peltier, W. R., Tan, N.,
1001 Contoux, C., Ramstein, G., Li, X., Zhang, Z., Guo, C., Nisancioglu, K. H., Zhang, Q., Li, Q., Kamae,
1002 Y., Chandler, M. A., Sohl, L. E., Otto-Bliesner, B. L., Feng, R., Brady, E. C., von der Heydt, A. S.,
1003 Baatsen, M. L. J. and Lunt, D. J.: The Pliocene Model Intercomparison Project Phase 2: large-scale
1004 climate features and climate sensitivity, Clim. Past, 16, 2095-2123, https://doi.org/10.5194/cp-16-
1005 2095-2020, 2020.
1006
1007 Haywood, A. M. and Valdes, P. J.: Modelling Middle Pliocene warmth: contribution of atmosphere,
1008 oceans and cryosphere, Earth Planet. Sc. Lett., 218, 363–377, doi:10.1016/S0012-821X(03)00685-X,
1009 2004.
1010
1011 Hunter, S. J., Haywood, A. M., Dolan, A. M. and Tindall, J. C.: The HadCM3 contribution to PlioMIP
1012 phase 2, Clim. Past, 15, 1691-1713, https://doi.org/10.5194/cp-15-1691-2019, 2019.
1013
1014 Hopcroft, P. O., Ramstein, G., Pugh, T.A.M., Hunter, S. J., Murguia-Flores, F., Quiquet, A., Sun, Y.,
1015 Tan, N. and Valdes, P. J.: Polar amplification of Pliocene climate by elevated trace gas radiative
1016 forcing, Proceedings of the National Academy of Sciences, DOI: 10.1073/pnas.2002320117, 2020
1017
1018 Howell, F. W., Haywood, A. M., Otto-Bliesner, B. L., Bragg, F., Chan, W.-L., Chandler, M. A.,
1019 Contoux, C., Kamae, Y., Abe-Ouchi, A., Rosenbloom, N. A., Stepanek, C., and Zhang, Z.: Arctic sea
1020 ice simulation in the PlioMIP ensemble, Clim. Past, 12, 749-767, https://doi.org/10.5194/cp-12-749-
1021 2016, 2016.
1022
1023 Kuhlbrodt, T., Jones, C. G., Sellar, A. et al.: The low resolution version of HadGEM3 GC3.1:
1024 Development and evaluation for global climate, JAMES, 10: 2865-2888,
1025 https://doi.org/10.1029/2018MS001370, 2018.
1026
1027 Li, X. Y., Jiang, D. B., Tian, Z. P., and Yang, Y. B.: Mid-Pliocene
1028 global land monsoon from PlioMIP1 simulations, Palaeogeogr. Palaeocl., 512, 56-70,
1029 https://doi.org/10.1016/j.palaeo.2018.06.027, 2018.
1030
1031 Lunt, D. J., Bragg, F., Chan, W.-L., Hutchinson, D. K., Ladant, J.-B., Morozova, P., Niezgodzki, I.,
1032 Steinig, S., Zhang, Z., Zhu, J., Abe-Ouchi, A., Anagnostou, E., de Boer, A. M., Coxall, H. K.,
1033 Donnadieu, Y., Foster, G., Inglis, G. N., Knorr, G., Langebroek, P. M., Lear, C. H., Lohmann, G.,
1034 Poulsen, C. J., Sepulchre, P., Tierney, J. E., Valdes, P. J., Volodin, E. M., Dunkley Jones, T., Hollis,
1035 C. J., Huber, M. and Otto-Bliesner, B. L.: DeepMIP: model intercomparison of early Eocene climatic

https://doi.org/10.5194/cp-2021-40
Preprint. Discussion started: 21 April 2021

optimum (EECO) large-scale climate features and comparison with proxy data, Clim. Past, 17, 203-227, https://doi.org/10.5194/cp-17-203-2021, 2021.

Martin, G. M. et al.: The HadGEM2 family of Met Office Unified Model climate configurations. Geosci. Model Dev. 4, 723-757. https://doi.org/10.5194/gmd-4-723-2011, 2011.

McClymont, E. L., Ford, H. L., Ho, S. L., Tindall, J. C., Haywood, A. M., Alonso-Garcia, M., Bailey, I., Berke, M. A., Littler, K., Patterson, M. O., Petrick, B., Peterse, F., Ravelo, A. C., Risebrobakken, B., De Schepper, S., Swann, G. E. A., Thirumalai, K., Tierney, J. E., van der Weijst, C., White, S., Abe-Ouchi, A., Baatsen, M. L. J., Brady, E. C., Chan, W.-L., Chandan, D., Feng, R., Guo, C., von der Heydt, A. S., Hunter, S., Li, X., Lohmann, G., Nisancioglu, K. H., Otto-Bliesner, B. L., Peltier, W. R., Stepanek, C. and Zhang, Z.: Lessons from a high-CO2 world: an ocean view from ~3 million years ago, Clim. Past, 16, 1599–1615, https://doi.org/10.5194/cp-16-1599-2020, 2020.

Menary, M. B., Kuhlbrodt, T., Ridley, J. et al.: Pre-industrial control simulations with HadGEM3-GC3.1 for CMIP6, JAMES, 10: 3049–3075, https://doi.org/10.1029/2018MS001495, 2018.

Moran, K., Backman, J., Brinkhuis, H., et al.: The Cenozoic palaeoenvironment of the Arctic Ocean, Nature, 441, 601-605, https://doi.org/10.1038/nature04800, 2006.

Lunt, D. J., Haywood, A. M., Schmidt, G. A., Salzmann, U., Valdes, P. J., Dowsett, H. J. and Loptson, C. A.: On the causes of mid-Pliocene warmth and polar amplification, EPSL, 321-322, 128-138, doi:10.1016/j.epsl.2011.12.042, 2012

Lunt, D. J., Huber, M., Anagnostou, E., Baatsen, M. L. J., et al.: The DeepMIP contribution to PMIP4: experimental design for model simulations of the EECO, PETM, and pre-PETM (version 1.0), Geosci. Model Dev., 10, 889-901, doi:10.5194/gmd-10-889-2017, 2017.

Polyak, L., Alley, R. B., Andrews, J. T., Brigham-Grette, J., Cronin, T. M., Darby, D. A., Dyke, A. S., Fitzpatrick, J. J., Funder, S., Holland, M., Jennings, A. E., Miller, G. H., O'Regan, M., Savelle, J., Serreze, M., St. John, K., White, J. W. C., and Wolff, E.: History of sea-ice in the Arctic, Quaternary Sci. Rev., 29, 1757-1778, doi:10.1016/j.quascirev.2010.02.010, 2010.

Pound, M. J., Tindall, J., Pickering, S. J., Haywood, A. M., Dowsett, H. J., and Salzmann, U.: Late Pliocene lakes and soils: a global data set for the analysis of climate feedbacks in a warmer world, Clim. Past, 10, 167-180, https://doi.org/10.5194/cp-10-167-2014, 2014.

https://doi.org/10.5194/cp-2021-40
Preprint. Discussion started: 21 April 2021

1073 Prahl, F. G. and S. G. Wakeham: Calibration of unsaturation patterns in long-chain ketone
1074 compositions for palaeotemperature assessment, Nature, 320, 367-369, 1987.
1075
1076 Ridley, J., Blockley, E., Keen, A. B. et al.: The sea ice model component of HadGEM3-GC3.1, GMD,
1077 11: 713-723, https://doi.org/10.5194/gmd-11-713-2018, 2017
1078
1079 Siahaan, A., and Walton, J.: The low resolution version of HadGEM3 GC3.1: Development and
1080 evaluation for global climate, JAMES, 10, 2865-2888, https://doi.org/10.1029/2018MS001370, 2018.
1081
1082 Salzmann, U., Dolan, A. M., Haywood, A. M., Chan, W.-L., Voss, J., Hill, D., Abe-Ouchi, A., Otto-
1083 Bliesner, B., Bragg, F. J., Chandler, M. A., Contoux, C., Dowsett, H. J., Jost, A., Kamae, Y.,
1084 Lohmann, G., Lunt, D. J., Pickering, S. J., Pound, M. J., Ramstein, G., Rosenbloom, N. A., Sohl, L.,
1085 Stepamek, C., Ueda, H. and Zhang, Z.: Challenges in quantifying Pliocene terrestrial warming
1086 revealed by data-model discord, Nat. Clim. Chang., 3, 969-974, https://doi.org/10.1038/nclimate2008,
1087 2013.
1088
1089 Salzmann, U., Haywood, A. M., Lunt, D. J., Valdes, P. J. and Hill, D. J.: A new global biome
1090 reconstruction and data-model comparison for the Middle Pliocene, Global Ecol. Biogeogr, 17, 432–
1091 447, https://doi.org/10.1111/j.1466-8238.2008.00381.x, 2008.
1092
1093 Sellar, A. A., Jones, C. G., Mulcahy, J. P., Tang, Y., Yool, A., Wiltshire, A., et al.: UKESM1:
1094 Description and evaluation of the U.K. Earth System Model, JAMES, 11,
1095 https://doi.org/10.1029/2019MS001739, 2019.
1096
1097 Smith, D. M., Screen, J. A., Deser, C., Cohen, J., Fyfe, J. C., García-Serrano, J., Jung, T., Kattsov, V.,
1098 Matei, D., Msadek, R., Peings, Y., Sigmond, M., Ukita, J., Yoon, J.-H., and Zhang, X.: The Polar
1099 Amplification Model Intercomparison Project (PAMIP) contribution to CMIP6: investigating the
1100 causes and consequences of polar amplification, GMD, 12, 1139-1164, https://doi.org/10.5194/gmd-
1101 12-1139-2019, 2019.
1102
1103 Storkey, D., Megann, A., Mathiot, P. et al.: UK Global Ocean GO6 and GO7: A traceable hierarchy
1104 of model resolutions, GMD, 11: 3187-3213, https://doi.org/10.5194/gmd-11-3187-2018, 2017
1105
1106 Tierney, J. E., Poulsen, C. J., Montañez, I. P., Bhattacharya, T., Feng, R., Ford, H. L., Hönisch, B.,
1107 Inglis, G. N., Petersen, S. V., Sagoo, N., Tabor, C. R., Thirumalai, K., Zhu, J., Burls, N. J., Foster, G.
1108 L., Goddéris, Y., Huber, B. T., Ivany, L. C., Turner, S. K., Lunt, D. J., McElwain, J. C., Mills, B. J.

https://doi.org/10.5194/cp-2021-40
Preprint. Discussion started: 21 April 2021

1109 W., Otto-Bliesner, B. L., Ridgwell, A. and Zhang, Y. G.: Past climates inform our future, Science,
1110 370, 6517, eaay3701, DOI:10.1126/science.aay3701, 2020.
1111
1112 Tindall, J. C. and Haywood, A. M.: Modelling the mid-Pliocene warm period using HadGEM2, Glob.
1113 Planet. Chang, 186, https://doi.org/10.1016/j.gloplacha.2019.103110, 2020.
1114
1115 Valdes, P. J., Armstrong, E., Badger, M. P. S., Bradshaw, C. D., Bragg, F., Crucifix, M., Davies-
1116 Barnard, T., Day, J. J., Farnsworth, A., Gordon, C., Hopcroft, P. O., Kennedy, A. T., Lord, N. S.,
1117 Lunt, D. J., Marzocchi, A., Parry, L. M., Pope, V., Roberts, W. H. G., Stone, E. J., Tourte, G. J. L.,
1118 and Williams, J. H. T.: The BRIDGE HadCM3 family of climate models: HadCM3@Bristol v1.0,
1119 Geosci. Model Dev., 10, 3715-3743, https://doi.org/10.5194/gmd-10-3715-2017, 2017.
1120
1121 Walters, D., Baran, A. J., Boutle, I., Brooks, M., Earnshaw, P., Edwards, J., Furtado, K., Hill, P.,
1122 Lock, A., Manners, J., Morcrette, C., Mulcahy, J., Sanchez, C., Smith, C., Stratton, R., Tennant, W.,
1123 Tomassini, L., Van Weverberg, K., Vosper, S., Willett, M., Browse, J., Bushell, A., Carslaw, K.,
1124 Dalvi, M., Essery, R., Gedney, N., Hardiman, S., Johnson, B., Johnson, C., Jones, A., Jones, C.,
1125 Mann, G., Milton, S., Rumbold, H., Sellar, A., Ujiie, M., Whitall, M., Williams, K., and Zerroukat,
1126 M.: The Met Office Unified Model Global Atmosphere 7.0/7.1 and JULES Global Land 7.0
1127 configurations, Geosci. Model Dev., 12, 1909-1963, https://doi.org/10.5194/gmd-12-1909-2019,
1128 2019.
1129
1130 Williams, C. J. R., Guarino, M.-V., Capron, E., Malmierca-Vallet, I., Singarayer, J. S., Sime, L. C.,
1131 Lunt, D. J., and Valdes, P. J.: CMIP6/PMIP4 simulations of the mid-Holocene and Last Interglacial
1132 using HadGEM3: comparison to the pre-industrial era, previous model versions and proxy data, Clim.
1133 Past, 16, 1429-1450, https://doi.org/10.5194/cp-16-1429-2020, 2020.
1134
1135 Williams, K. D., Copsey, D., Blockley, E. W., Bodas-Salcedo, A., Calvert, D., Comer, R., Davis, P.,
1136 Graham, T., Hewitt, H. T., Hill, R., Hyder, P., Ineson, S., Johns, T. C., Keen, A. B, Lee, R. W.,
1137 Megann, A., Milton, S. F., Rae, J. G. L., Roberts, M. J., Scaife, A. A., Schiemann, R., Storkey, D.,
1138 Thorpe, L., Watterson, I. G., Walters, D. N., West, A., Wood, R. A., Woollings, T., and Xavier, P. K.:
1139 The Met Office Global Coupled Model 3.0 and 3.1 (GC3.0 and GC3.1) Configurations, JAMES, 10,
1140 357-380, https://doi.org/10.1002/2017MS001115, 2017.
1141
1142 Zelinka, M. D., Myers, T. A., McCoy, D. T., Po-Chedley, S., Caldwell, P. M., Ceppi, P., Klein, S. A.
1143 and Taylor, K. E.: Causes of higher climate sensitivity in CMIP6 models, Geophys. Res. Lett., 47,
1144 e2019GL085782. https://doi.org/10.1029/2019GL085782, 2020.
1145

https://doi.org/10.5194/cp-2021-40
Preprint. Discussion started: 21 April 2021


Climate of the Past Discussions

Zhang, R., Yan, Q., Zhang, Z. S., Jiang, D., Otto-Bliesner, B. L., Haywood, A. M., Hill, D. J., Dolan, A. M., Stepanek, C., Lohmann, G., Contoux, C., Bragg, F., Chan,W.-L., Chandler, M. A., Jost, A., Kamae, Y., Abe-Ouchi, A., Ramstein, G., Rosenbloom, N. A., Sohl, L., and Ueda, H.: Mid-Pliocene East Asian monsoon climate simulated in the PlioMIP, Clim. Past, 9, 2085-2099, https://doi.org/10.5194/cp-9-2085-2013, 2013.

Zhang, R., Zhang, Z. S., Jiang, D. B., Yan, Q., Zhou, X., and Cheng, Z. G.: Strengthened African summer monsoon in the mid-Piacenzian, Adv. Atmos. Sci., 33, 1061-1070, https://doi.org/10.1007/s00376-016-5215-y, 2016.

Zhang, Z., Li, X., Guo, C., Otterå, O. H., Nisancioglu, K. H., Tan, N., Contoux, C., Ramstein, G., Feng, R., Otto-Bliesner, B. L., Brady, E., Chandan, D., Peltier, W. R., Baatsen, M. L. J., von der Heydt, A. S., Weiffenbach, J. E., Stepanek, C., Lohmann, G., Zhang, Q., Li, Q., Chandler, M. A., Sohl, L. E., Haywood, A. M., Hunter, S. J., Tindall, J. C., Williams, C. J. R., Lunt, D. J., Chan, W.-L. and Abe-Ouchi, A.: Mid-Pliocene Atlantic Meridional Overturning Circulation simulated in PlioMIP2, Clim. Past, 17, 529-543, https://doi.org/10.5194/cp-17-529-2021, 2021.

Zhu, J., Poulsen, C. J. and Otto-Bliesner, B. L.: High climate sensitivity in CMIP6 model not supported by paleoclimate, Nat. Clim. Chang, 10, 378-379, https://doi.org/10.1038/s41558-020-0764-6, 2020.